Nat. Hazards Earth Syst. Sci., 10, 275–294, 2010
www.nat-hazards-earth-syst-sci.net/10/275/2010/

Natural Hazards and Earth System Sciences

Unfolding the procedure of characterizing recorded ultra low frequency, kHZ and MHz electromagnetic anomalies prior to the L'Aquila earthquake as pre-seismic ones - Part 2

K. Eftaxias[1], **G. Balasis**[2], **Y. Contoyiannis**[1], **C. Papadimitriou**[1], **M. Kalimeri**[1], **L. Athanasopoulou**[1], **S. Nikolopoulos**[3], **J. Kopanas**[1], **G. Antonopoulos**[1], **and C. Nomicos**[4]

[1]Section of Solid State Physics, Department of Physics, University of Athens, Panepistimiopolis, Zografos, 15784, Athens, Greece
[2]Institute for Space Applications and Remote Sensing, National Observatory of Athens, Metaxa and Vas. Pavlou, Penteli, 15236, Athens, Greece
[3]Centre de Recherche de l'ICM, INSERM UMRS 975 - CNRS UMR 7225, Hopital de la Pitie-Salpetriere, Paris, France
[4]Department of Electronics, Technological Educational Institute of Athens, Ag. Spyridonos, Egaleo, 12210, Athens, Greece

Received: 23 September 2009 – Revised: 7 January 2010 – Accepted: 12 January 2010 – Published: 16 February 2010

Abstract. Ultra low frequency-ULF (1 Hz or lower), kHz and MHz electromagnetic (EM) anomalies were recorded prior to the L'Aquila catastrophic earthquake (EQ) that occurred on 6 April 2009. The detected anomalies followed this temporal scheme. (i) The MHz EM anomalies were detected on 26 March 2009 and 2 April 2009. The kHz EM anomalies were emerged on 4 April 2009. The ULF EM anomaly was appeared from 29 March 2009 up to 3 April 2009. The question effortlessly arises as to whether the observed anomalies before the L'Aquila EQ were seismogenic or not. The main goal of this work is to provide some insight into this issue. More precisely, the main aims of this contribution are threefold: How can we recognize an EM observation as pre-seismic one? We aim, through a multidisciplinary analysis to provide some elements of a definition. How can we link an individual EM anomaly with a distinctive stage of the EQ preparation process? The present analysis is consistent with the hypothesis that the kHz EM anomalies were associated with the fracture of asperities that were distributed along the L'Aquila fault sustaining the system, while the MHz EM anomalies could be triggered by fractures in the highly disordered system that surrounded the backbone of asperities of the activated fault. How can we identify precursory symptoms in an individual EM precursor that indicate that the occurrence of the EQ is unavoidable? We clearly state that the detection of a MHz EM precursor does not mean that the occurrence of EQ is unavoidable; the abrupt emergence of kHz EM emissions indicate the fracture of asperities. The observed ULF EM anomaly supports the hypothesis of a relationship between processes produced by increasing tectonic stresses in the Earth's crust and attendant EM interactions between the crust and ionosphere. We emphasize that we attempt to specify not only whether or not a single EM anomaly is pre-seismic in itself, but mainly whether a combination of emergent ULF, MHz and kHz EM anomalies could be characterized as pre-earthquake.

1 Introduction

A catastrophic EQ occurred on 6 April 2009 (01 h 32 m 41 s UTC) in central Italy (42.35° N–13.38° E) with magnitude M_W=6.3. The majority of the damage occurred in the city of L'Aquila, the medieval capital city of the Abruzzo region (Fig. 1).

EM anomalies of a broad frequency range, namely, from ULF (1 Hz or lower), kHz up to MHz (Figs. 2–5), were detected by the sensors located at a mountainous site of Zante island (37.76° N–20.76° E) in the Ionian Sea (western Greece) (Fig. 1) prior to the L'Aquila EQ.

"Are there credible EQ precursors?" is a question debated in the science community. Herein, based on a multidisciplinary approach, we examine the possible seismogenic origin of the detected EM anomalies.

An EQ is a sudden mechanical failure in the Earth's crust, which has heterogeneous structures. It is reasonable to expect that its preparatory process has various facets which may be observed before the final catastrophe through seismic,

Correspondence to: K. Eftaxias
(ceftax@phys.uoa.gr)

Published by Copernicus Publications on behalf of the European Geosciences Union.

Fig. 1. In the map the location of the Zante station and the epicentre of the L'Aquila EQ are shown.

geochemical, hydrological and EM changes (Uyeda et al., 2009). Therefore, the science of EQ prediction should, from the start, be multi-disciplinary (Uyeda et al., 2009). Possible precursory phenomena include changes in seismic velocities, tilt and strain precursors, hydrologic phenomena, chemical emissions and EM signals (Rundle et al., 2003). Herein, we focus on EM precursors.

Pre-seismic EM emissions have been internationally observed before large EQs (Hayakawa and Fujinawa, 1994; Hayakawa, 1999; Hayakawa et al., 1999; Smirnova et al., 2001; Hayakawa and Molchanov, 2002; Varotsos, 2005; Pulinets and Boyarchuk, 2005; Ida et al., 2005; Eftaxias et al., 2007a, Molchanov and Hayakawa, 2008). These seismo-EM signals may be conveniently classified into the following two major classes (Uyeda et al., 2009 and references therein):

(i) *Direct EM precursors*: EM signals believed to be emitted from within the focal zones.

EM precursors of a broad frequency range, from low frequency (1 Hz or lower), kHz up to MHz, have been internationally reported before large EQs (Uyeda et al., 2009 and references therein).

Seismic electric signals (SES), which are low frequency transient anomalies in telluric current, precede EQs, with a lead time from several hours to a few months (Varotsos, 2005). Pressure stimulated polarization currents (PSPC), which are emitted from solid containing electric dipoles upon a gradual increase of the pressure (or stress) can be a plausible source among other for SES generation (Varotsos, 2005). This emission occurs when the stress reaches a critical value which does not have to coincide with the fracture stress. The electro-kinetic effect, also called *streaming potential*, can also be a plausible source for SES EM emissions (Uyeda et al., 2009 and references therein). Freund and his colleagues have also proposed a mechanism for ULF electric signals (Freund et al., 2006): when rocks are stressed, peroxy links break, releasing h* charge carriers which are highly mobile and can flow out of the stressed sub-volume.

On the other hand, when a material is strained, intense acoustic and EM emissions, ranging from MHz to kHz, are produced by opening cracks when failure is approached. A stressed rock behaves like a stress-EM transformer. These precursors are detectable both at laboratory and geological scale (Hayakawa and Fujinawa, 1994; Hayakawa, 1999; Hayakawa et al., 1999; Gershenzon and Bambakidis, 2001; Hayakawa and Molchanov, 2002; Bahat et al., 2005; Eftaxias et al., 2007a; Muto et al., 2007; Hadjicontis et al., 2007). Studies on the small (laboratory) scale reveal that the MHz EM radiation appears earlier than the kHz one, while the kHz EM emission is launched from 97% up to 100% of the corresponding failure strength (Eftaxias et al., 2002 and references therein). On the large (geological) scale, intense MHz and kHz EM emissions precede EQs that: (i) occurred in land (or near coast-line), (ii) were strong (magnitude 6 or larger), (iii) were shallow (Eftaxias et al., 2002, 2004, 2006, 2007b; Kapiris et al., 2004a, b; Karamanos et al., 2006). Their lead time is ranged from a few days to a few hours. Importantly, the MHz radiation precedes the kHz one at geophysical scale, as well (Eftaxias et al., 2002; Kapiris et al., 2004a; Contoyiannis et al., 2005). Notice that a complete sequence of SES, MHz and kHz EM anomalies have been observed one after the other in a series of significant EQs that occurred in Greece (Eftaxias et al., 2000, 2002; Karamanos et al., 2006; Papadimitriou et al., 2008). We argue that the detected MHz and kHz EM anomalies were emitted from the focal area of the L'Aquila EQ.

(ii) *Indirect EM precursors*: EM phenomena believed to be rooted in seismo-ionospheric coupling

Ample experimental evidence suggests that the preparation of EQ induces a lithosphere-atmosphere-ionosphere (LAI) coupling mechanism where EM precursory phenomena are originated (Hayakawa and Fujinawa, 1994; Gokhberg et al., 1995; Hayakawa, 1999; Hayakawa et al., 1999; Hayakawa and Molchanov, 2002; Pulinets et al., 2003; Pulinets and Boyarchuk, 2005, Molchanov and Hayakawa, 2008). The regional but substantially *large-scale* changes over seismically active areas before the seismic shock are mapped into the ionosphere. Both natural and artificial EM signals propagate in the Earth-ionosphere waveguide. Any change in the lower ionosphere due to an induced pre-seismic LAI-coupling may result in significant changes in the signal propagation-received at a station. We suggest that the recorded ULF EM anomaly prior to the L'Aquila EQ fits in this category.

Despite fairly abundant circumstantial evidence pre-seismic EM signals have not been adequately accepted as real physical quantities. It seems appropriate at this point to admit that there may be legitimate reasons for the critical views. The degree to which we can predict a phenomenon is often measured by how well we understand it. However, many questions about fracture processes remain standing. Kossobokov (2006) *emphasizes that no scientific prediction is possible without exact definition of the anticipated phenomenon and the rules which define clearly in advance of it whether the prediction is conformed or not.*

We pay attention to the fact that the time lags between pre-earthquake EM anomalies and EQs are different for different types of precursors. The remarkable asynchronous appearance of precursors indicates that they refer to different stages of EQ preparation process. Moreover, it implies a different mechanism for their origin. Scientists ought to attempt to link the available various EM observations that appear one after the other to the consecutive processes occurring in Earth's crust. The comprehensive understanding of EM precursors in terms of physics is an important research target. In our opinion that is a path to achieve more sufficient knowledge of last stages of the EQ preparation process and thus more sufficient short-term EQ prediction. A seismic shift in thinking towards basic science will result a renaissance of strict definitions and systematic experiments in the field of EQ prediction (Cyranoski, 2004).

1.1 Data collection

Our main tool is the monitoring of the fractures, which occur in the focal area before the final breakup, by recording their MHz-kHz EM emissions. Since 1994, a station has been functioning at a mountainous site of Zante island in the Ionian Sea (western Greece) (Fig. 1) with the following configuration: (i) six loop antennas recording the three components (EW, NS, and vertical) of the variations of the magnetic field at 3 kHz and 10 kHz, respectively; (ii) two vertical $\lambda/2$ electric dipole antennas recording the electric field variations at 41 and 54 MHz, respectively. Clear MHz-kHz EM anomalies have been detected over periods ranging from a few days to a few hours before shallows land-based (or near coast-line) EQs with magnitude 6 or larger since the installation of the station. Recent results indicate that the observed precursors contain characteristic pre-fracture features (Eftaxias et al., 2002, 2004, 2006, 2007b, 2009; Kapiris et al., 2004a, b; Contoyiannis et al., 2005, 2008; Karamanos et al., 2006; Kalimeri et al., 2008; Papadimitriou et al., 2008).

In order to detect indirect ionospheric precursors we have installed two Short Thin Wire Antennas (STWA) of 100-m length each, lying in the Earths surface in the EW and NS directions, respectively. The analog sensitive device that measures the potential difference in each antenna includes a low-pass active filter with a cut-off frequency of 1 Hz. Thus, the system records ultra low frequency (<1 Hz) electric anomalies. Clear ULF EM anomalies have been detected a few days before shallows land-based (or near coast-line) EQs with magnitude 6 or larger since the installation of the station (Eftaxias et al., 2000, 2002, 2004; Karamanos et al., 2006). All the EM time-series are sampled once per second.

We stress that the experimental arrangement affords us the possibility to determine not only whether or not a single EM anomaly is pre-seismic in itself, but also whether a combination of ULF, MHz and kHz EM anomalies can be characterized as pre-seismic.

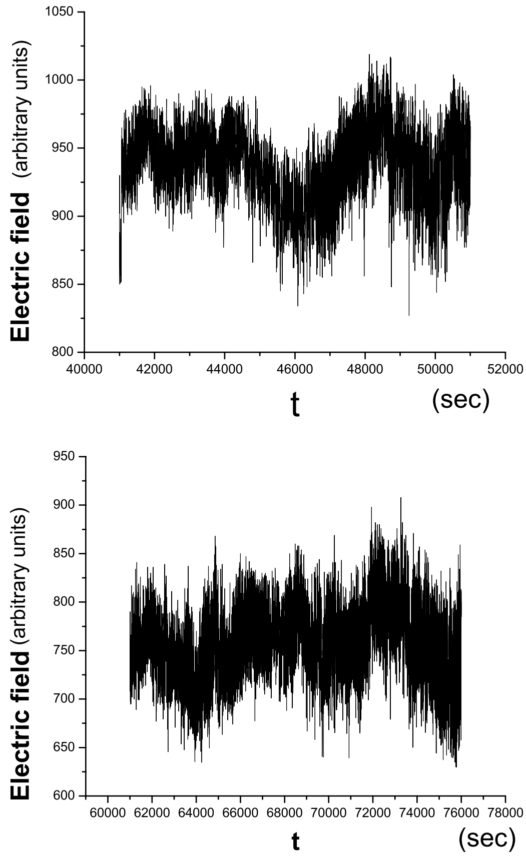

Fig. 2. The two excerpts of the 41 MHz electric field strength time series which show anti-persistency and can be described as analogous to a thermal continuous (second order) phase transition. The two critical time intervals emerged on 26 March 2009 (upper panel) and 2 April 2009 (lower panel), respectively.

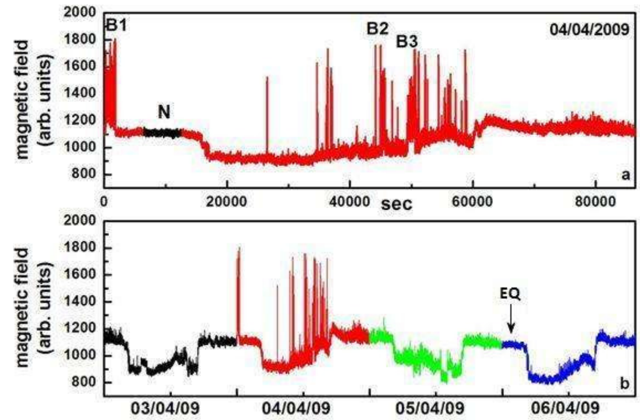

Fig. 3. **(a)** A sequence of strong EM bursts at 10 kHz emerged on 4 April 2009. **(b)** These anomalies appeared over a quiescence period concerning the detection of EM disturbances. A segment from the EM background (N) and three excerpts of the detected strong kHz EM activity (B1, B2, B3) have been marked in the time series of 4 April 2009.

1.2 EM anomalies observed prior to the L'Aquila earthquake

The L'Aquila EQ was a very shallow land-based event with magnitude 6.3. Notice that various methods show that the top of the activated fault is located from 3.0 km up to 0 km bellow from the Earths surface (Walters et al., 2009). The observed anomalies followed this temporal scheme:

Two MHz electric anomalies appeared on 26 March 2009 and 2 April 2009 (Fig. 2).

A sequence of strong impulsive kHz magnetic bursts was emerged on 4 April 2009 (Fig. 3). Figure 4 shows magnified images of three kHz EM bursts and an excerpt of noise marked in Fig. 3.

No co-seismic KHz-MHz EM anomalies were observed before the L'Aquila EQ by our group.

In this field of research the repeatability of results is desirable. The Chinese (Qian et al., 1994) and Greek (Eftaxias, et al., 2000, 2002; Contoyiannis et al., 2005; Contoyiannis and Eftaxias, 2008) experience can be summarized in the following points: the frequency band of the detected EM anomalies is quite wide; anomalies are detected earlier in the electric field than in the magnetic field.

The ULF anomaly appeared from 29 March 2009 up to 3 April 2009 (Fig. 5). Importantly, based on very low frequency (kHz) radio sounding, Rozhnoi et al. (2009) and Biagi et al. (2009) have observed ionospheric perturbations in the time interval 2–8 days before the L'Aquila EQ.

We note that all the recorded EM anomalies have been obtained during a quiet period in terms of magnetic storms and solar flares activity.

1.3 The aim of this work

We have yet pointed out that pre-seismic EM signals have not been adequately accepted as real physical quantities (Uyeda et al., 2009). Some open questions in this field of research are:

How can we recognize an EM observation as a pre-seismic one? We wonder whether sufficient and necessary criteria have been established that permit the characterization of an EM observation as an EM precursor.

How can we link an individual EM precursor with a distinctive stage of the EQ preparation process?

How can we identify crucial precursory symptoms in an EM observation that indicate that the occurrence of the EQ is unavoidable?

Here we shall study the possible seismogenic origin of EM anomalies recorded prior to the L'Aquila EQ within the frame work of the above questions.

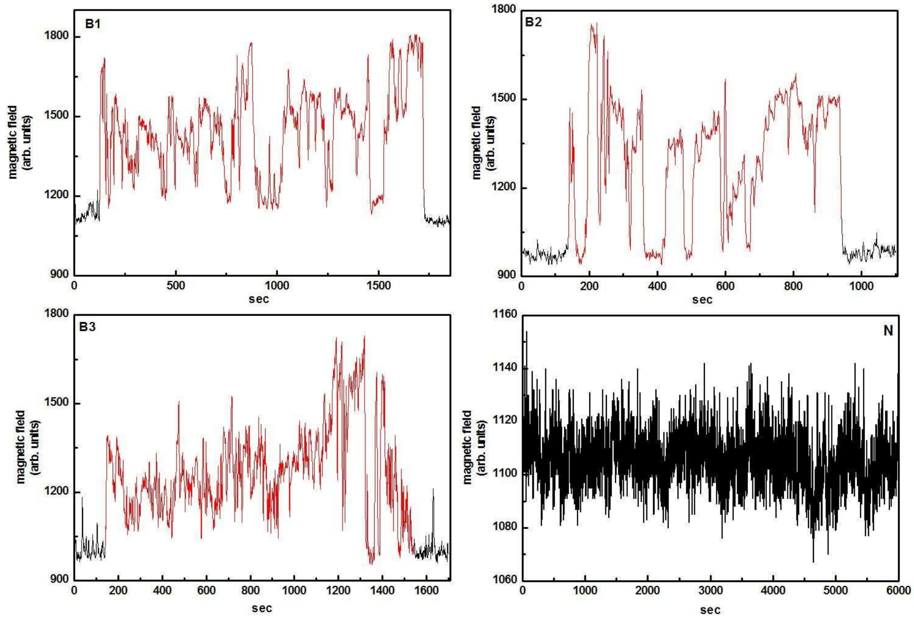

Fig. 4. Magnified images of the excerpts N, B1, B2, and B3 that are shown in Fig. 3.

2 A two stages model of EQ preparation in terms of MHz-kHz EM emission

An important challenge in this field of research is to distinguish characteristic epochs in the evolution of the EM response to geodynamic processes occurring in the Earths upper crust and identify them with the equivalent stages in the EQ preparation process. Any result of such an approach, either a success or a failure, clarifies our knowledge about seismic processes supporting or rejecting the underlying conceptions.

We recall that an important feature, observed both on laboratory and geophysical scale, is that the MHz radiation precedes the kHz one (Eftaxias et al., 2002 and references therein). Recently, we proposed that the pre-earthquake MHz and kHz EM anomalies obey the following two-stage model (Kapiris et al., 2004a; Contoyiannis et al., 2005; Eftaxias et al., 2006, 2007b; Papadimitriou et al., 2008).

The pre-seismic MHz EM emission is thought to be due to the fracture of the highly heterogeneous system that surrounds the family of large high-strength asperities distributed along the fault sustaining the system.

The kHz EM radiation is due to the fracture of the asperities themselves.

By the end of this paper we will argue that the emergent MHz and kHz EM anomalies prior to the L'Aquila EQ also follow the aforementioned two stages model.

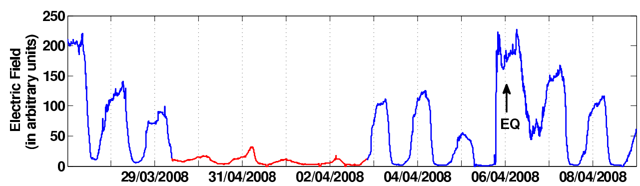

Fig. 5. The ULF EM anomaly which was detected from 29 March 2009 up to 3 April 2009 is shown in red. Over this time interval the bay-like morphology of the daily ULF data is absent.

3 How can we recognize a ULF, MHz or kHz EM anomaly as a candidate precursor?

We emphasize that we attempt to establish a MHz or kHz EM anomaly as a seismogenic one based on the above mentioned two stages model. From the beginning, for our reader's convenience, we briefly present our proposal.

3.1 Focus on MHz EM anomalies

The interplay between the heterogeneities and the stress field is responsible for the existence of stationary anti-persistent behavior during the fracture of a highly heterogeneous system, namely, the appearance of a nonlinear negative feedback in the fracture mechanism which "kicks" the opening cracks away from extremes. Thus, a candidate MHz EM precursor should show stationary anti-persistent behaviour (see Sect. 4). The aforementioned behaviour justifies the following proposal: the fracture in highly heterogeneous systems can be described via an analogy with thermal continuous phase transition. Thus, a candidate MHz EM precursor should be described by means of a second order phase transition in equilibrium (see Sect. 4).

The above mentioned crucial footprints, namely, antipersistency and criticality, are not found in quiet MHz EM observations.

3.2 Focus on kHz EM anomalies

Fracture surfaces were found to be self-affine following the persistent fractional Brownian motion (fBm) model over a wide range of length scales. Thus, a candidate kHz EM precursor should behave as a temporal fractal following the persistent fBm model (see Sect. 5.2).

The characteristic of a kHz EM precursor rooted in an activated fault should be related to the irregularity of fault geometry. Importantly, the spatial roughness of fracture surfaces has been interpreted as a universal indicator of surface fracture, weakly dependent on the nature of the material and on the failure mode. Thus, the kHz EM anomaly should have temporal profile with roughness which is in harmony with the universal spatial roughness of fracture surfaces (see Sect. 5.3).

The aspects of self-affine nature of faulting and fracture have been well-established. Consequently, by means of self-affinity, the candidate kHz EM precursor should behave as a "reduced image" of the regional seismicity, and a " magnified image" of laboratory seismicity by means of acoustic and EM emissions (see Sect. 6).

The aforementioned key signatures are not found in quiet kHz EM observations.

Notice that in Part 1of this contribution (Eftaxias et al., 2009b) we have concentrated on the detected kHz EM anomaly. We have analyzed the data successively in terms of various concepts of entropy and information theory including, Shannon n-block entropy, conditional entropy, entropy of the source, Kolmogorov-Sinai entropy, T-entropy, approximate entropy, fractal spectral analysis, R/S analysis and detrended fluctuation analysis. We argue that this analysis reliably distinguishes the candidate kHz EM precursor from the noise. The appearance of candidate kHz EM precursors are combined by a simultaneous appearance of a significantly higher level of organization (or lower complexity, lower uncertainty, higher predictability, higher compressibility) in comparison to that of the background, and persistency.

3.3 Focus on ULF EM anomalies

The daily ULF EM data presents a bay-like behaviour during quiet periods. The records during the quiet periods refer to the Earth-ionosphere waveguide propagation of natural EM emission that depends mostly on sources rooted in atmosphere and ionosphere (see p. 46 in ref. Gokhberg et al., 1995). Any change in the lower ionosphere due to an induced pre-seismic LAI-coupling may result in significant changes in the signal propagation-received at a station. Thus, the emergence of an ULF anomaly is recognized by a strong perturbation of the characteristic bay-like morphology in the chain of daily ULF data (see Sect. 7).

4 On the possible seismogenic origin of the observed MHz EM anomalies

Fracture process in heterogeneous materials is characterized by fundamental properties. Especially, such a fracture process is characterized by anti-persistency, and can be described in analogy with a thermal continuous second order phase transition. These two crucial footprints should be mirrored on the associated MHz EM precursor (Kapiris et al., 2004a, Contoyiannis et al., 2005; Contoyiannis and Eftaxias, 2008).

In natural rocks at large length scales there are long-range anti-correlations, in the sense that a high value of a rock property, e.g. threshold for breaking, is followed by a low value and vice versa (Kapiris et al., 2004, Contoyiannis et al., 2005 and references therein; Contoyiannis and Eftaxias, 2008). Failure nucleation begins to occur at a region where the resistance to rupture growth has the minimum value. An EM event is emitted during this fracture. The fracture process continues in the same weak region until a much stronger region is encountered in its neighbourhood. When this happens, fracture stops, and thus the emitted EM emission sieges. The stresses are redistributed, while the applied stress in the focal area increases. A new population of cracks nucleates in the weaker of the unbroken regions, and thus a new EM event appears, and so on. In summary, the interplay between the heterogeneities and the stress field in the focal area should be responsible for the appearance of antipersistency in a pre-seismic MHz EM time series (Kapiris et al., 2004a; Contoyiannis et al., 2005, 2009; Contoyiannis and Eftaxias, 2008). In the following, we will show that the detected MHz activity before the L'Aquila EQ is really characterized by anti-persistency.

Physically, the presence of anti-persistency implies a set of EM fluctuations tending to induce stability to the system, essentially the existence of a non-linear negative feedback mechanism that "kicks" the opening rate of cracks away from extremes. The existence of such a mechanism leads to the next step: in analogy to the study of critical phase transitions in statistical physics, it has been proposed that the fracture of heterogeneous materials can be described in analogy with a thermal continuous second order phase transition in equilibrium (Herrmann and Roux, 1990; Sornette, 2004; Contoyiannis et al., 2005 and references therein). We will show that the observed MHz EM anomalies can be described such as critical phenomenon by means of the recently introduced Method of Critical Fluctuations (MCF) (Contoyiannis and Diakonos, 2000; Contoyiannis et al., 2002). We note that MHz EM anomalies detected prior to significant EQs in Greece follow the aforementioned antipersistent and critical behaviour (Contoyiannis et al., 2005, 2009; Contoyiannis and Eftaxias, 2008).

4.1 The method of critical fluctuations

The MCF, which constitutes a statistical method of analysis for the critical fluctuations in systems that undergo a continuous phase transition at equilibrium, has been recently introduced (Contoyiannis and Diakonos, 2000; Contoyiannis et al., 2002). The authors have shown that the fluctuations of the order parameter ϕ, that correspond to successive configurations of critical systems at equilibrium, obey a dynamical law of intermittency which can be described in terms of a 1-d nonlinear map. The invariant density $\rho(\phi)$ for such a map is characterized by a plateau which decays in a super-exponential way (see Fig. 1 in Contoyiannis and Diakonos, 2000). The exact dynamics at the critical point can be determined analytically for a large class of critical systems introducing the so-called critical map (Contoyiannis and Diakonos, 2000). For small values of ϕ, this critical map can be approximated as

$$\phi_{n+1} = \phi_n + u\phi_n^z + \epsilon_n \tag{1}$$

The shift parameter ϵ_n introduces a non-universal stochastic noise: each physical system has its characteristic "noise", which is expressed through the shift parameter ϵ_n. For thermal systems the exponent z is introduced, which is related to the isothermal critical exponent δ by $z = \delta + 1$.

The plateau region of the invariant density $\rho(\phi)$ corresponds to the laminar region of the critical map where fully correlated dynamics takes place (Contoyiannis et al., 2005 and references therein). The laminar region ends when the second term in Eq. (1) becomes relevant. However, due to the fact that the dynamical law (1) changes continuously with ϕ, the end of the laminar region cannot be easily defined based on a strictly quantitative criterion. Thus, the end of the laminar region should be generally treated as a variable parameter.

Based on the foregoing description of the critical fluctuations, the MCF develops an algorithm permitting the extraction of the critical fluctuations, if any, in a recorded time series. The important observation in this approach is the fact that the distribution $P(l)$ of the laminar lengths l of the intermittent map (1) in the limit $\epsilon_n \to 0$ is given by the power law (Contoyiannis et al., 2002)

$$P(l) \sim l^{-p_l} \tag{2}$$

where the exponent p_l is connected with the exponent z via $p_l = \frac{z}{z-1}$. Therefore the exponent p_l is related to the isothermal exponent δ by

$$p_l = 1 + \frac{1}{\delta} \tag{3}$$

where $\delta > 0$.

Inversely, the existence of a power law such as relation (2), accompanied by a plateau form of the corresponding density $\rho(\phi)$, is a signature of underlying correlated dynamics similar to critical behavior (Contoyiannis and Diakonos, 2000; Contoyiannis et al., 2002).

We emphasize that it is possible in the framework of universality, which is characteristic of critical phenomena, to give meaning to the exponent p_l beyond the thermal phase transitions (Contoyiannis et al., 2002).

Up to now, the MCF has been applied on numerical experiments of thermal systems (Ising models) (Contoyiannis et al., 2002), kHz EM pre-seismic signals (Contoyiannis et al., 2005, 2009; Contoyiannis and Eftaxias 2008), and electrocardiac signals from biological tissues (Contoyiannis et al., 2004).

The MCF is directly applied to time series or to segments of time series which appear to have a cumulative stationary behavior. The main aim of the MCF is to estimate the exponent p_l. The distribution of the laminar lengths, l, of fluctuations included in a stationary window is fitted by the relation:

$$P(l) \sim l^{-p_2} e^{-p_3 l} \tag{4}$$

If p_3 is zero, then p_2 is equal to p_l. Practically, as p_3 approaches zero, then p_2 approaches p_l and the laminar lengths tend to follow a power-law type distribution. So, we expect a good fit to Eq. (4) with $p_2 > 1$ and $p_3 \approx 0$ if the system is in a critical state (Stanley, 1999). In terms of physics this behaviour means that the system is characterized by a "strong criticality", e.g., the laminar lengths tend to follow a power-law type distribution: during this critical time window the opening cracks (EM emitters) are well correlated even at large distances (Stanley, 1999).

We stress that when the exponent p_2 is smaller than one, then, independently of the p_3-value, the system is not in a critical state. Generally, the exponents p_2, p_3 have a competitive character, namely, when the exponent p_2 decreases the associated exponent p_3 increases (they are mirror images of each other). To be more precise, as the exponent p_2 ($p_2 < 1$) is close to 1 and simultaneously the exponent p_3 is close to zero, then the system is in a sub-critical state. As the system moves away from the critical state, then the exponent p_2 further decreases while simultaneously p_3 increases, reinforcing in this way the exponential character of the laminar length distribution: the EM fluctuations show short range correlations. In this way, we can identify the deviation from the critical state (Stanley et al., 1999).

In summary, the research of criticality in natural systems could be quantitatively accomplished by estimating the values of only two parameters, namely the exponents p_2 and p_3.

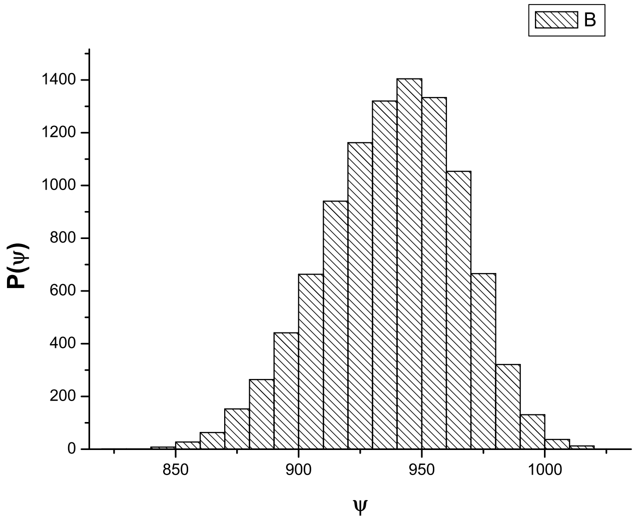

Fig. 6. The distribution of the amplitude (order parameter) $P(\psi)$ of the electric fluctuations included in the critical window which was appeared on 26 March 2009 (see Fig. 2, upper panel).

4.2 Application of the MCF method to the detected pre-seismic MHz EM radiation prior to the L'Aquila EQ

As it was said, two critical MHz EM anomalies were detected on 26 March 2009 and 2 April 2009 prior to the EQ. In (Contoyiannis et al., 2009) we have shown that the anomaly recorded on 2 April 2009 can be described as analogous to a thermal continuous phase transition, and has anti-persistent behaviour. These features imply that this candidate precursor could be triggered by fractures in the highly disordered system that surrounded the backbone of asperities of the activated fault (Contoyiannis et al., 2005).

Herein, we study the critical MHz anomaly that emerged on 26 March 2009 (Fig. 2a). The critical time interval includes approximately 10000 points (Fig. 2a). The stationary behaviour of this critical window has been checked by estimating the mean value and the standard deviation for various time intervals in the critical window, all having a common origin (Contoyiannis et al., 2005). Notice that we have shown that the amplitude of the recorded electric time series, or equivalently the output of the detector, behaves as *order parameter* (Contoyiannis et al., 2005). The symbol ψ symbolizes the order parameter in this particular case under study. The corresponding distribution of the amplitude (order parameter) $P(\psi)$ in the candidate critical window is shown in Fig. 6.

The next step is to produce the distribution of the laminar lengths, l. The laminar length gives the stay time within the laminar region. More precisely, the laminar lengths are described by the lengths of the sub-sequences in the time series that result from successive ψ-values obeying the condition $\psi_o \le \psi \le \psi_l$, where ψ_o is the fixed point and the end of the laminar region ψ_l is a variable parameter. Notice that when the distribution is asymmetric, as in the case under study, the side of distribution which decays more abruptly denotes the fixed point ψ_o (Pingel et al., 1999; Diakonos et al., 1999). Thus, the fixed point is $\psi_o = 1000$ (see Fig. 6). Consequently, the end of the laminar region ψ_l "runs" the points on the other side of distribution. In the following, using the fitting function (4), we estimate the critical exponents p_2, p_3 for different ψ_l-values. In order to avoid end effects we ignore the values coming from the end points of the distribution. Figure 7b shows an example of the distribution of the laminar lengths for a given end point ($\psi_l = 940$). The function (4) fits the data with $p_2 = 1.48$ and $p_3 = 0.009$, while the quality of fitting is excellent ($r^2 = 0.998$). In Fig. 7a the exponents p_2, p_3 are plotted against the end points ψ_l. Figure 7a reveals that the majority of the p_2 values are greater than 1 and the corresponding p_3-values close to zero for all end points of laminar regions. This finding indicates that all the trajectories are critical and carry essentially the same information about the dynamical term. The system is characterized by a "strong criticality". The laminar lengths tend to follow a power-law type distribution: during this critical time window the opening cracks (EM emitters) are well correlated even at large distances.

Figure 8 shows the corresponding critical behaviour of the MHz EM fluctuations which appeared on 2 April 2009 (Fig. 2b). This group of EM fluctuations also shows a strong criticality. The associated analysis by means of MCF has been presented in details in (Contoyiannis et al., 2009).

For the purpose of comparison we analyze two time intervals of the background EM noise, which have been obtained on 28 March 2009 and 4 April 2009, correspondingly. These two time intervals do not exhibit any criticality. In the first time interval the associated distribution of the laminar lengths of fluctuations is fitted by the function (4) with $p_2 = 0.55$ and $p_3 = 0.22$ (see Fig. 9, upper panel). In the second time interval the data are fitted by the function (4) with $p_2 = 0.81$ and $p_3 = 0.13$ (see Fig. 9, lower panel). These results imply that the laminar lengths do not follow a power law distribution; the included EM fluctuations show short range correlations indicating that the underlying dynamics is rather chaotic than deterministic (Contoyiannis et al., 2004). A situation like this is compatible with a noisy random EM background.

In this way we have discriminated the two critical windows which were appeared in a MHz EM time series prior to the seismic event under study.

4.3 The anti-persistent behaviour of the candidate EM precursor

The exponent Hurst H characterizes the persistent/anti-persistent properties of the signal (Eftaxias et al., 2009b and references therein). The range $0<H<0.5$ indicates an

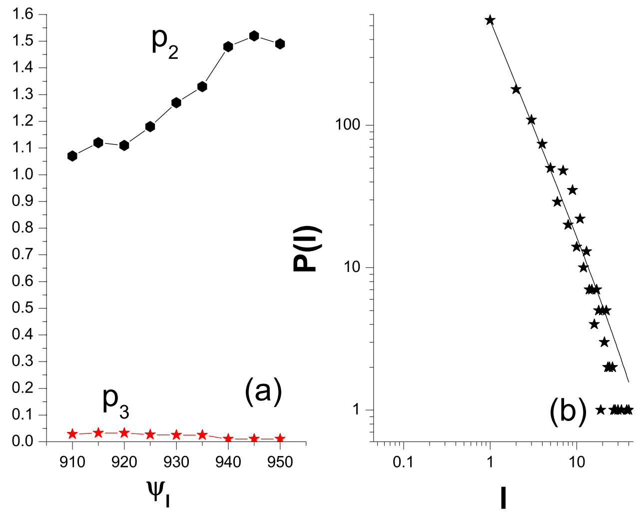

Fig. 7. The figure refers to the critical window which appeared in 41 MHz EM time series on 26 March 2009 (see Fig. 2, upper panel). The Fig. 7a shows the exponents p_2 and p_3 versus the end of laminar region ψ_1. We observe that the majority of the p_2 values is greater than 1 and the corresponding p_3-values are close to zero for all the end points of laminar regions ψ_1. This finding suggests that the laminar lengths tend to follow a power-law type distribution. The underlying physical background is that during this critical time window the opening cracks (EM emitters) are well correlated even at large distances. The Fig. 7b shows an example of the distribution of the laminar lengths for a given end point ($\psi_1 = 940$). In this case, the function $P(l) \sim l^{-p_2} e^{-p_3 l}$ fit the data with $p_2 = 1.48$ and $p_3 = 0.009$, while the quality of fitting is excellent ($r^2 = 0.998$).

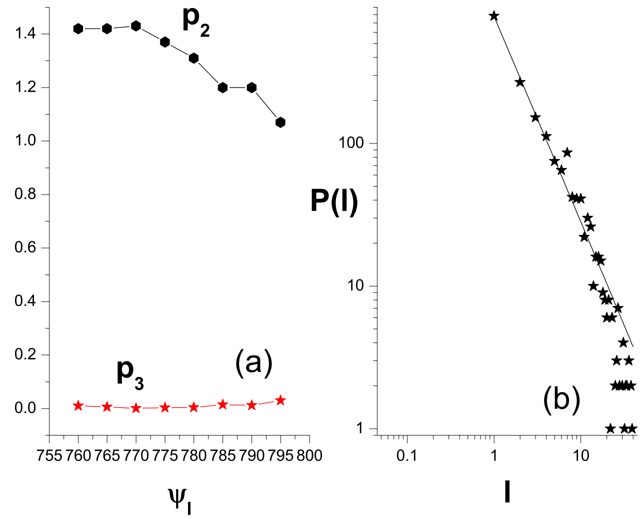

Fig. 8. The figure refers to the critical window which appeared in 41 MHz EM time series on 2 April 2009 (see Fig. 2, lower panel). The Fig. 8a shows the exponents p_2 and p_3 versus the end of laminar region ψ_1. We observe that the majority of the p_2 values is greater than 1 and the corresponding p_3-values are close to zero for all the end points of laminar regions ψ_1. This finding suggests that the laminar lengths tend to follow a power-law type distribution. The underlying physical background is that during this critical time window the opening cracks (EM emitters) are well correlated even at large distances. The distribution of the laminar lengths for a given end point ($\psi_1 = 770$) is shown in Fig. 8b. The function $P(l) \sim l^{-p_2} e^{-p_3 l}$ fit the data with $p_2 = 1.43$ and $p_3 = 0.008$, while the quality of fitting is excellent ($r^2 = 0.997$).

anti-persistency so that increases in the fluctuations within a time internal are likely to be followed by decreases in the following time internal, and conversely. On the contrary, the range $0.5<H<1$ ($2<\beta<3$) indicates persistent behavior. This means that increases in the fluctuations within a time internal are likely to be followed by increases in the next internal, so the system starts to govern by a positive feedback process. Sammis and Sornette (2002) have presented the most important mechanisms which are characterized by positive feedback.

Recently, we introduced the following connection between the exponents H and p_2 (Contoyiannis et al., 2005):

$$H = 2 - \frac{3}{2} p_2 \tag{5}$$

As we see from this equation, the allowed range of p_2 values for a second-order phase transition, i.e., $p_2 > 1$, leads to the condition $H < 0.5$ which indicates the existence of an anti-persistent mechanism. It was found that Eq. (5) is valid only if the exponent p_2 lies in the interval $1 < p_2 < 1.5$ (Contoyiannis et al., 2005). Figures 7 and 8 show that the p_2 values associated with the emergent two MHz EM precursors on 26 March 2009 and 2 April 2009 correspondingly obey the restriction $1 < p_2 < 1.5$, and thus show anti-persistency. As it was mentioned, the interplay between the heterogeneities and the stress field in the focal area could be responsible for the observed anti-persistent pattern.

The question naturally arises as to whether the appearance of criticality and anti-persistency is systematically observed. Recently, we have listed MHz EM activities recorded prior to nine significant EQs that have been occurred in-land (or near coast line) (Contoyiannis et al., 2009). All these precursors show anti-persistency and can be described in analogy with a thermal continuous second order transition.

A key-question concerns the physical mechanism that drives the heterogeneous system to its critical state. Combining the ideas of Levy statistics, non-extensive Tsallis statistics (Tsallis, 1988, 2009) and criticality on the one hand, and features included in the precursory MHz time series on the other, we argued that *a Levy-walk-type mechanism can drive the heterogeneous system to criticality* (Contoyiannis et al., 2008).

We conclude that two fundamental features of fracture of heterogeneous materials have been projected on the detected MHz EM activities. This finding supports the hypothesis that they are associated with the fracture process in the heterogeneous regime of the focal area.

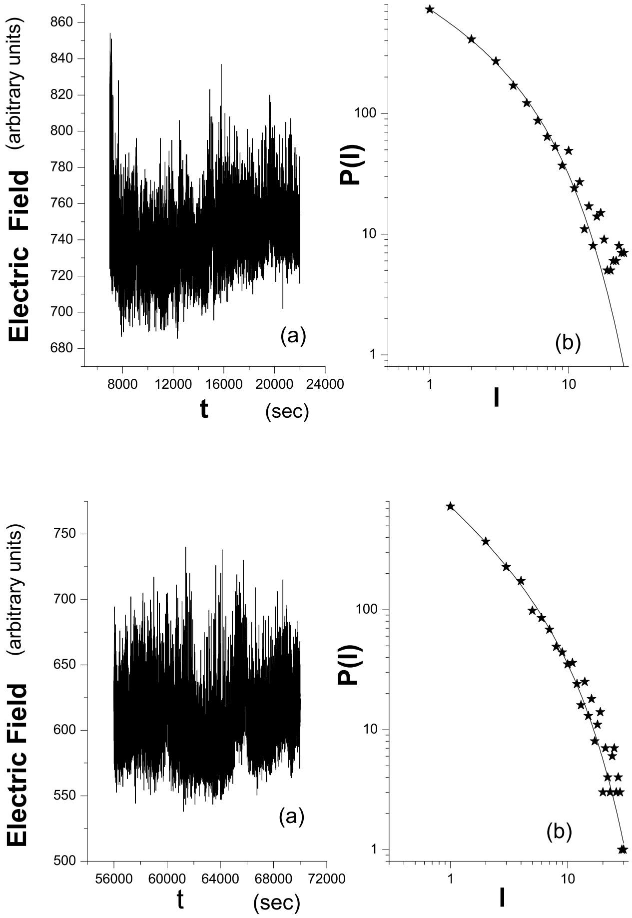

Fig. 9. The figure refers to two excerpts of the 41 MHz EM time series which do not exhibit any criticality. They have been recorded on 28 March 2009 (upper panel) and 4 April 2009 (lower panel), correspondingly. In the first time interval (upper panel) the distribution of the laminar lengths is fitted by the function $P(l) \sim l^{-p_2} e^{-p_3 l}$ with $p_2 = 0.55$ and $p_3 = 0.22$. In the second time interval (lower panel) the data are fitted with $p_2 = 0.81$ and $p_3 = 0.13$. Consequently, the laminar lengths do not follow a power law distribution. The electric fluctuations show short range correlations indicating that the underlying dynamics is rather chaotic than deterministic. A situation like this is compatible with a noisy random EM background.

4.4 Is the evolution towards global failure irreversible after the appearance of the MHz EM precursor?

A fundamental question that we ought to address is as follows. *Is the evolution towards global failure irreversible after the appearance of the MHz EM precursor?* We clearly state in (Contoyiannis et al., 2005) that the detection of a MHz EM precursor, which could be described in analogy with a thermal continuous second order transition and shows anti-persistent behaviour, does not mean that the occurrence of EQ is unavoidable. Its appearance reveals that the fracture of heterogeneous system in the focal area has been obstructed along the backbone of asperities that sustain the system. *The "siege" of strong asperities begins. The EQ will occur if and when the local stress exceeds the fracture stress of asperities*. We argue that the abrupt emergence of kHz EM emissions indicates the fracture of asperities and thus signalizes that the evolution of the process toward global failure is unavoidable (Kapiris et al., 2004a; Contoyiannis et al., 2005; Papadimitriou et al., 2008; Eftaxias, 2009). In our opinion, the appearance of a critical anti-persistent MHz EM anomaly is a *necessary* but not *sufficient* condition for the EQ occurrence. We have detected such MHz EM anomalies which, however, were not accompanied by a significant EQ. We emphasize that: (i) following the procedure, which has been reported in (Koulouras et al., 2009), we have excluded the possibility that these anomalies were related to magnetic storm activity or solar flare activity; (ii) the emergence of these MHz anomalies were not accompanied by the appearance of kHz and ULF EM anomalies. It is an open question whether these critical and anti-persistent "strange" anomalies were seismogenic ones or not.

5 Focus on the possible seismogenic origin of the detected kHz EM anomaly

In Part 1 of this communication (Eftaxias et al., 2009b) we focus on the detected kHz EM anomaly. We analyze the data successively in terms of various concepts of entropy and information theory, namely, Shannon n-block entropy, conditional entropy, entropy of the source, Kolmogorov-Sinai entropy, T-entropy, approximate entropy, fractal spectral analysis, R/S analysis and detrended fluctuations analysis. The application of the aforementioned procedure clearly recognizes and discriminates the candidate kHz EM precursors from the EM background in the region of the station. All the techniques suggest that the kHz EM anomaly is characterized by a significant lower complexity (or higher organization, lower uncertainty, higher predictability, higher compressibility), and strong persistency. The simultaneous appearance of both these two characteristics implies that the underlying fracture process is governed by a positive feedback mechanism (Sammis and Sornette, 2002). Such a mechanism is consistent with the anomalys being a precursor of an ensuing catastrophic event.

However, by the end of Part 1 (Eftaxias et al., 2009b) we conclude that the results of this multidisciplinary analysis by themselves are not sufficient to characterize the kHz EM anomalies as pre-earthquake ones. In our opinion they offer necessary but not sufficient criteria in order to recognize an emergent kHz EM anomaly as a precursory one. Much remains to be done to tackle systematically real pre-seismic EM precursors.

5.1 Our strategy

The Earth's crust is extremely complex. However, despite its complexity, there are several universally holding scaling relations (Eftaxias, 2009 and references therein). Such universal structural patterns of fracture and faulting process should be included into an associated EM precursor. Therefore, an important pursuit is to make a quantitative comparison between temporal fractal patterns possibly hidden in an emergent kHz EM anomaly on one hand and universal spatial fractal patterns of fracture surfaces on the other hand. Notice that Maslov et al. (1994) have formally established the relationship between spatial fractal behavior and long-range temporal correlations for a broad range of critical phenomena. They showed that both the temporal and spatial activity can be described as different cuts in the same underlying fractal. A self-organized critical process, as the source of the temporal power-laws, would further suggest that similar power-laws exist also for parameters in the spatial domain (Hansen and Schmittbuhl, 2003). Laboratory experiments support the consideration that both the temporal and spatial activity can be described as different cuts in the same underlying fractal. Characteristically, Ponomarev et al. (1997) have studied in the laboratory the temporal evolution of Hurst exponent for the series of distances H_r and time intervals H_t between consecutive acoustic emission events in rocks. Their analysis indicates that the changes of H_r and H_t with time occur in phase, while the relationship $H_r \approx H_t$ is valid.

From the early work of Mandelbrot (1982), much effort has been put into the statistical characterization of the resulting fractal surfaces in fracture processes: (i) fracture surfaces were found to be self-affine following the fractional Brownian motion (fBm) model over a wide range of length scales. (ii) The spatial roughness of fracture surfaces has been interpreted as a universal indicator of surface fracture, weakly dependent on the nature of the material and on the failure mode.

Therefore, two questions naturally arise as to whether the kHz EM activity detected prior to the L'Aquila EQ constitutes a temporal fractal following the fBm model, and has a temporal profile with roughness which is in harmony with the universal spatial roughness of fracture surfaces.

Moreover, the aspects of self-affine nature of faulting and fracture have been well-established. Consequently, two additional questions arise as to whether the kHz EM precursor statistically behaves a " reduced image" of the regional seismicity (Huang and Turcotte, 1988), and a "magnified image" of laboratory seismicity. In the subsequent subsections we attempt to answer the above mentioned crucial questions.

5.2 Signatures of fractional-Brownian-motion nature of faulting and fracture in the candidate kHz EM precursor

Ample experimental and theoretical evidence supports the existence of a fractional Brownian motion scheme: (i) kinematic or dynamic source inversions of EQs suggest that the final slip (or the stress drop) has a heterogeneous spatial distribution over the fault (see among others Gusev, 1992; Bouchon, 1997; Peyrat et al., 2001). (ii) Power spectrum analysis of the fault surface suggests that heterogeneities are observed over a large range of scale lengths (see Power et al., 1987, in particular Fig. 4). (iii) Investigators of the EQ dynamics have already pointed out that the fracture mechanics of the stressed crust of the Earth forms self-similar fault patterns, with well-defined fractal dimensionalities (Barriere and Turcotte, 1991). (iv) Following the observations of the self-similarity in various length scales in the roughness of the fractured solid surfaces, Chakrabarti et al. (1999) have proposed that the contact area distribution between two fractal surfaces follows a unique power law. (vi) Huang and Turcotte (1988) have pointed out that natural rock surfaces can be represented by fBm over a wide range.

If a time series is a temporal fractal then a power-law of the form $S(f) \propto f^{-\beta}$ is obeyed, with $S(f)$ the power spectral density and f the frequency. A pioneering work on fractal analysis of ULF emissions was made by Hayakawa et al. (1999). In Part 1 of this contribution (Eftaxias et al., 2009b) we shown that the emergent strong kHz EM fluctuations on 4 April 2009 follow the law $S(f) \propto f^{-\beta}$, while the β exponent takes high values, i.e., between 2 and 3. This finding indicates that the temporal profile of the observed EM bursts actually follows the fBm-model (Heneghan and McDarby, 2000). We review this analysis in Fig. 10.

In summary, the universal fBm profile of the fracture surfaces has been mirrored in the temporal profile of the kHz EM activity under study.

5.3 Footprints of universal roughness value of fracture surfaces in the kHz EM activity

The Hurst exponent, H, specifies the strength of the irregularity ("roughness") of the fBm surface topography: the fractal dimension is calculated from the relation $D = (2 - H)$ (Heneghan and McDarby, 2000).

The height-height correlation function

$$\Delta h(r) = < [h(r + \Delta r) - h(r)]_r^{1/2}$$

computed along a given direction is found to scale as $\Delta h \sim (\Delta r)^H$. The "roughness" exponent H expresses the tendency for $dh = [dh(x)/dx]dx$ to change sign. When $1/2 < H < 1$, the sign tends not to change. The value $H = 1$ is an upper bound reached when the "roughness" of the fault is minimum, in other words, a differentiable surface topography corresponds to $H = 1$. When $H = 1/2$, the sign of dh

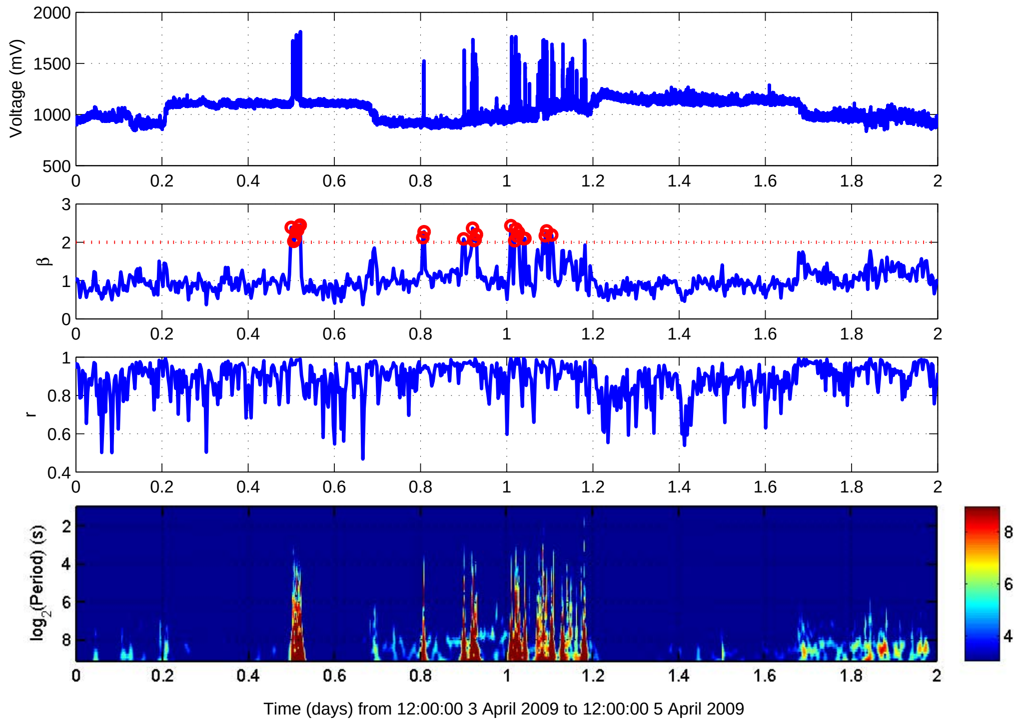

Fig. 10. From top to bottom are shown the 10 kHz time series, spectral exponents β, linear correlation coefficients r, and the wavelet power spectrum from 3 to 5 April 2009. The red dashed line in the plot marks the transition from anti-persistent to persistent behavior. We observe that in the emerged strong kHz EM bursts the coefficient r takes values very close to 1, i.e., the fit to the power-law $S(f) \propto f^{-\beta}$ is excellent. This means that the fractal character of the kHz EM activity is solid. The β exponent takes high values, i.e., between 2 and 3. This reveals that the candidate precursor follows the persistent Fractional Brownian motion model.

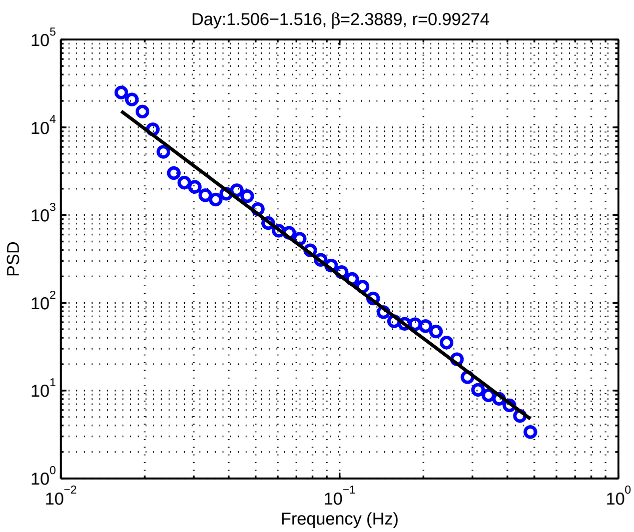

Fig. 11. The log-log representation of the function $S(f) \propto f^{-\beta}$ into an excerpt of the recorded kHz EM anomaly, namely EM burst B1 (see Figs. 3a and 4), is shown. The associated β exponent is equal to 2.39, which leads to $H = 0.7$. This means that the roughness of the profile of the kHz EM timeseries is in harmony with the universal roughness of fracture surfaces.

changes randomly, and the corresponding surface possesses no spatial correlations. For $0 < H < 1/2$ there is a tendency for the sign to change (anticorrelation). The value $H = 0$ is a lower bound; as H tends towards 0 trends are more rapidly reversed giving a very irregular look.

We paid attention to the fact that the Hurst exponent $H \sim 0.7 - 0.8$ has been interpreted as a universal indicator of surface fracture, weakly dependent on the nature of the material and on the failure mode (Lopez and Schmittbuhl, 1998; Hansen and Schmittbuhl, 2003; Ponson et al., 2006; Mourot et al., 2006; Zapperi et al., 2005).

In Part 1 of this work (Eftaxias et al., 2009b) we showed that the “roughness” of the profile of the kHz EM time series, as it is represented by the Hurst exponent, is distributed around the value 0.7. This result has been verified by means of both fractal spectral analysis and R/S analysis.

Importantly, the surface roughness of a recently exhumed strike-slip fault plane has been measured by three independent 3-D portable laser scanners (Renard et al., 2006). This fault plane refers to the Vuache fault, near Annecy in the French Alps. Statistical scaling analyses show that the striated fault surface exhibits self-affine scaling invariance that can be described by a scaling roughness exponent, H_1=0.7 in the direction of slip. Figure 11 shows the log-log representation of $S(f) \propto f^{-\beta}$ into a characteristic excerpt of the recorded kHz EM anomaly, namely the EM burst B1. The associated β exponent is equal to 2.39, which leads to $H = 0.7$. We recall that the β exponent is related to the Hurst exponent, H, by the formula $\beta = 2H + 1$, for the fBm (Heneghan and McDarby, 2000).

We conclude that the universal spatial roughness of fracture surfaces nicely coincides with the roughness of the temporal profile of the kHz EM anomaly that was emerged on 4 April 2009, i.e., a few tens of hours prior to the L'Aquila EQ.

The observed low "roughness" in the recorded kHz EM bursts is consistent with the following physical picture. As the two rough surfaces of the activated fault relatively move, the "details" in the topography of two surfaces are gradually removed, thus there is an increase in the population of larger asperities with time with respect to that of small asperities. Simultaneously, contacts become more closely spaced. In this way a high Hurst exponent decreases the number but increases the size of contacts/kHz EM events. In summary, the observed more or less regularity in the temporal profile of the recorded kHz EM anomaly is in harmony with the fracture of a family of large, strong and closely spaced asperities.

Systematic high-resolution laboratory experiments have been performed by Ohnaka and Shen (1999) on the nucleation of propagating slip failure on pre-existing faults having different surface roughness to demonstrate how the size scale and duration on shear rupture nucleation are affected by geometric irregularity of the rupturing surfaces. The authors conclude that the rougher the rupturing surfaces, the greater the timescales of rupture nucleation are. In the frame of this study, the observed short duration of the recorded kHz EM bursts is consistent with the estimated low "roughness".

6 The activation of the L'Aquila fault as a "reduced self-affine image" of regional natural seismicity and a "magnified self-affine image" of laboratory seismicity

The aspect of self-affine nature of faulting and fracture is widely documented from field observations, laboratory experiments, and studies of failure precursors on the small (laboratory) and large (EQ) scale (Mandelbrot, 1982; Huang and Turcotte, 1988; Turcotte, 1997; Rabinivitch et al., 2001; Rundle et al., 2003; Sornette, 2004; Muto et al., 2007). This fundamental aspect bridges the activation of a single fault with the regional seismicity on one hand and laboratory seismicity on the other hand. In the following we examine whether the kHz EM precursor verifies this prospect. More precisely, we try to show that the activation of the L'Aquila fault is a reduced self-affine image of the regional seismicity and a self-affine magnified image of laboratory seismicity. Importantly, Huang and Turcotte (1988) have suggested that the statistics of regional seismicity could be merely a macroscopic reflection of the physical processes in EQ source. For the aforementioned purpose, we are based on a model for EQ dynamics coming from a non-extensive Tsallis formulation (Tsallis, 1988, 2009). This model has been proposed by Solotongo-Costa and Posadas (2004). Silva et al. (2006) have revised this model. We also are based on the Gutenberg-Richter (G-R) magnitude-frequency relationship for EQs (Gutenberg and Richter, 1954).

6.1 The L'Aquila fault activation as a reduced self-affine image of the regional seismicity

The EQ dynamics model proposed by Solotongo-Costa and Posadas (2004) is starting from first principles. The authors assume that: the mechanism of relative displacement of fault plates is the main cause of EQs. The space between fault planes is filled with the residues of the breakage of the tectonic plates, from where the faults have originated. The motion of the fault planes can be hindered not only by the overlapping of two irregularities of the profiles, but also by the eventual relative position of several fragments. Thus, the mechanism of triggering EQs is established through the combination of the irregularities of the fault planes on one hand and the fragments between them on the other hand. The fragments size distribution function comes from a nonextensive Tsallis formulation, starting from first principles, i.e., a nonextensive formulation of the maximum entropy principle. This approach leads to a G-R type law for the magnitude distribution of EQs:

$$\log(N(m>)) = \log N + \left(\frac{2-q}{1-q}\right) \cdot \log\left[1 + \alpha(q-1)\cdot(2-q)^{(1-q)/(q-2)} 10^{2m}\right] \quad (6)$$

where N is the total number of EQs, $N(m>)$ the number of EQs with magnitude larger than m, and $m \approx \log(\varepsilon)$. α is the constant of proportionality between the EQ energy, ε and the size of fragment, r. More precisely, Solotongo-Costa and Posadas assume that $\varepsilon \propto r$. We clarify that the entropic index q describes the deviation of Tsallis entropy from the traditional Shannon one.

Silva et al. (2006) have subsequently revised this model considering the current definition of the mean value, i.e., the so-called q-expectation value. They also suggested a Gutenberg-Richter type law, which provides an excellent fit to seismicities, too:

$$\log(N_{>m}) = \log N + \left(\frac{2-q}{1-q}\right) \cdot \log\left[1 - \left(\frac{1-q}{2-q}\right)\left(\frac{10^{2m}}{\alpha^{2/3}}\right)\right] \quad (7)$$

Herein α is the constant of proportionality between the EQ energy, ε, and the size of fragment, r.

We emphasize that the proposed non-extensive G-R type laws (6) and (7) provide an excellent fit to seismicities generated in various large geographic areas usually identified as "seismic regions", each of them covering many geological

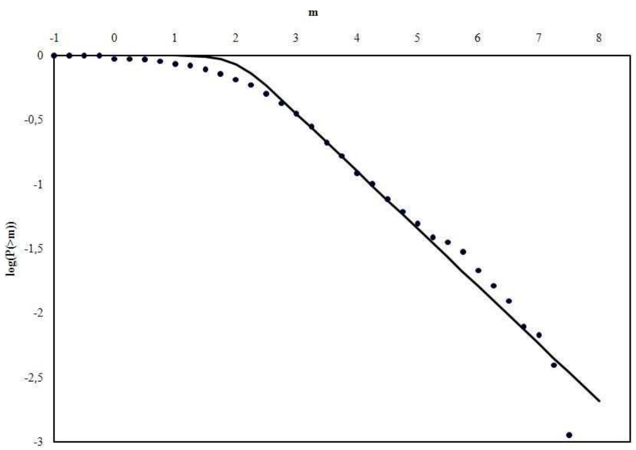

Fig. 12. We use formula (7), which quantitatively describes the nonextensive model for EQ dynamics in terms of regional seismicity, to calculate the relative cumulative number of kHz "electromagnetic earthquakes", $P(>m)$, included in the whole precursory phenomenon depicted in Fig. 3. There is an agreement of formula (7) with the data. The associated nonextensive q-parameter has value 1.82.

faults: the q-values are restricted in the narrow region from 1.60 to 1.71 (Solotongo-Costa and Posadas, 2004; Silva et al., 2006; Vilar et al., 2007). Notice that the magnitude-frequency relationships for EQs (6) and (7) do not say anything about a specific activated fault (EQ). Interestingly, Hallgass et al. (1997) have emphasized that what is lacking is the description of what happened locally, i.e., as a consequence of a single event. The candidate kHz EM precursor refers to a specific (L'Aquila) fault.

When a material is strained, EM emissions are produced by opening cracks. Thus, in the frame of the above-mentioned nonextensive models for EQ dynamics, a precursory sequence of EM bursts occurs when there is fracture of the fragments that fill the space between the irregular fault planes of the activated individual fault. In the following, we study whether the statistics of regional seismicity could be merely a macroscopic self-affine reflection of the L'Aquila EQ, as it has been early suggested by Huang and Turcotte (1988). Recently, we have examined this issue in terms of Solotongo-Costa and Posadas approach (Eftaxias, 2009a). Herein, we investigate the universality by means of the revised model for EQ dynamics which has been introduced by Silva et al. (2006) and quantitatively described by Eg. (7).

We regard as amplitude A of a candidate "fracto-EM fluctuation" the difference $A_{\text{fem}}(t_i) = A(t_i) - A_{\text{noise}}$, where A_{noise} is the background (noise) level of the EM time series. We consider that a sequence of k successively emerged "fracto-EM fluctuations" $A_{\text{fem}}(t_i)$, $i = 1, \ldots, k$ represents the EM energy released, ε, during the damage of a fragment. We shall refer to this as an "EM EQ". Since the squared amplitude of the fracto-EM emissions is proportional to their energy, the magnitude m of the candidate "EM EQ" is given by the relation

$$m = \log\varepsilon \sim \log\left(\sum [A_{\text{fem}}(t_i)]^2\right) \quad (8)$$

Figure 12 shows that Eq. (7) provides an excellent fit to the pre-seismic kHz EM experimental data incorporating the characteristics of nonextensivity statistics into the distribution of the detected precursory "EM EQs" on 4 April 2009. Herein, $N(m>)$ is the number of "EM EQs" with magnitude larger than m, $P(>m) = N(m>)/N$ is the relative cumulative number of "EM EQs" with magnitude larger than m, and α is the constant of proportionality between the EM energy released and the size of fragment. *The best-fit parameter for this analysis is given by* $q = 1.82$.

Figure 13 shows that Eq. (7) also provides an excellent fit to the "EM EQs" included in the EM burst B1 (see Figs. 3 and 4) with $q = 1.87$.

It is very interesting to observe the similarity in the q-values associated with the non-extensive Eq. (7) for: (i) seismicities generated in various large geographic areas, and (ii) the precursory sequence of "EM EQs" possibly associated with the activation of the L'Aquila fault. This finding indicates that the statistics of regional seismicity could be merely a macroscopic reflection of the physical processes in the EQ source, as it has been suggested by Huang and Turcotte (1988).

Remark: A very clear kHz EM precursor was emerged prior to the Athens (Greece) EQ (M=5.9) that occurred on 7 September 1999. Importantly, this precursor also follows Eq. (7) with $q = 1.80$ which is nicely close to that associated with the precursor of the L'Aquila EQ ($q = 1.82$).

We note that the estimated non-extensive q parameter is in full agreement with the upper limit $q < 2$ obtained from several studies involving the Tsallis non-extensive framework (Carvalho et al., 2008; Zunino et al., 2008). Moreover, it is in harmony with an underlying sub-extensive system, $q > 1$, verifying the emergence of strong interactions in the Earths crust during the EQ preparation process.

6.2 The activation of the L'Aquila fault as a "magnified self-affine image" of the laboratory seismicity

It would be helpful to have analyses of laboratory seismicities by means of nonextensive formulae (6) and (7), and thus to compare the corresponding q-values with the ones associated with the kHz EM activity under study. Unfortunately, this information is lacking. However, laboratory seismicities have been investigated in terms of the traditional Gutenberg-Richter (G-R) law, which is the best known scaling relation

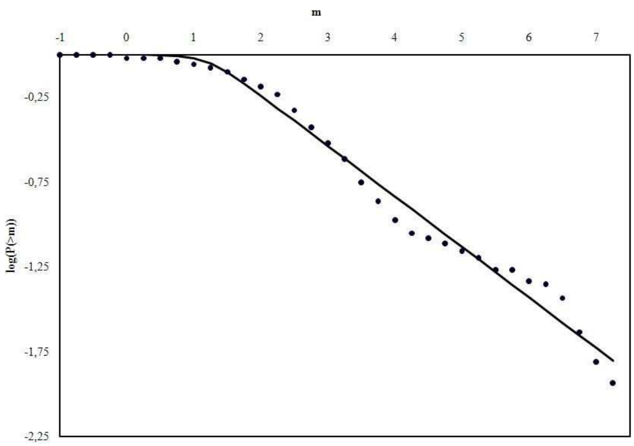

Fig. 13. We use formula (7), which quantitatively describes the nonextensive model for EQ dynamics in terms of regional seismicity, to calculate the relative cumulative number of kHz "electromagnetic earthquakes", $P(>m)$, included in the first burst (B1) depicted in Figs. 3a and 4. There is an agreement of formula (7) with the data. The associated nonextensive q-parameter has a value of 1.87.

for EQs: the cumulative number of EQ with magnitude greater than M is given by

$$\log N(>m) = \alpha - bm, \tag{9}$$

where $N(m>)$ is the cumulative number of EQs with a magnitude greater than m occurring in a specified area and time and b and α are constants. Due to the above mentioned reasons, we examine whether the traditional G-R law also describes the energy distribution of the kHz EM anomalies prior to the L'Aquila EQ.

In Fig. 14 we depict the quantity $N(>m)$ vs. "fracto-EM fluctuation" magnitude, m, where $N(>m)$ is the cumulative number of "fracto-EM fluctuations" with magnitude greater than m. The main part of this distribution is given by $\log N(>M) = \alpha - bm$, where $b = 0.52$.

We focus on the estimated value $b \sim 0.52$. There are increasing reports on premonitory decrease of b-value immediately before the global fracture. Characteristically, Lei and Satoh (2007), based on acoustic emission events recorded during catastrophic fracture of typical rock samples under differential compression, suggest that the pre-failure damage evolution is characterized by a dramatic decrease in b-value from ~ 1.5 to ~ 0.5 for hard rocks. Laboratory experiments in terms of acoustic emission performed by Ponomarev et al. (1997) also showed a significant fall of the observed b-values from ~ 1 to ~ 0.6 just before the global rupture. Rabinovitch et al. (2001) found that laboratory piezo-stimulated EM emission follows the G-R law with $b = 0.62$. Notice that the sequence of kHz EM fluctuations recorded prior to the Athens EQ obey the G-R distribution with $b = 0.62$.

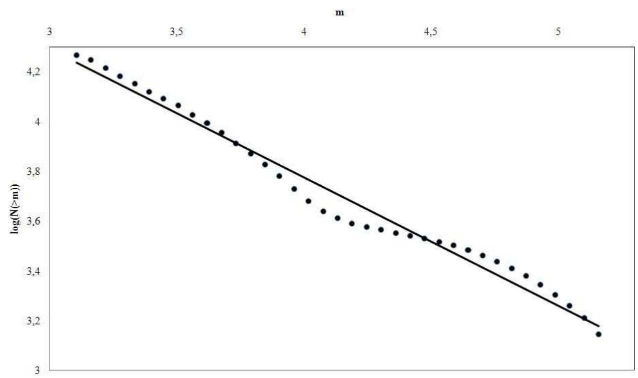

Fig. 14. Number of kHz "electromagnetic fluctuations" emerged on 4 April 2009 with a magnitude m higher than that given by the corresponding abscissa. The continuous line is the least squares fit the law $\log N(>m) = \alpha - bm$, where $b \sim 0.52$.

The above mentioned results verify that the activation of the L'Aquila fault behaves as a magnified self-affine image of the laboratory seismicity.

On the other hand, it is known that a significant decrease of b-value takes place before EQs, as well: foreshock sequences and main shocks are characterized by a much smaller exponent compared to aftershocks, $b \sim 1$. This evidence further verifies that the activation of the L'Aquila fault behaves as a reduced self-affine image of the regional natural seismicity.

The b-value represents a statistical measurement of the relative abundance of large and small EQs in the group. The estimated low b-value means that a high fraction of the total observed "EM-EQs" prior to the L'Aquila EQ occurs at higher magnitudes. This finding is in consistency with the estimated high and low values of β and H exponents, respectively.

6.3 Evidence of fractional-Brownian-motion-type asperity model for EQ generation in candidate the kHz EM emission associated with the L'Aquila EQ

De Rubeis et al. (1996) and Hallgass et al. (1997) have introduced a self-affine asperity model for the seismicity that mimics the fault friction by means of two fractional Brownian profiles that slide one over the other. An EQ occurs when there is an overlap of the two profiles representing the two fault faces and its energy is assumed proportional to the overlap surface. This model exhibits a good interpretation by means of the Gutenberg-Richter law of the seismicity generated in a large geographic area usually identified as "seismic region", covering many geological faults, on a global sense.

Hallgass et al. (1997) have stated that "what is lacking is the description of what happened locally, i.e., as a consequence of a single event, from both the temporal and the spatial point of view". In this section, we focus on the activation of a single, namely L'Aquila fault. In the frame of the proposed self-affine asperity model for EQ dynamics the fracture of an intersection between the two fractional Brownian profiles of a single fault is accompanied by the launch of an individual kHz EM burst ("EM-EQ"). Therefore, a vital question is whether the sequence of the observed kHz EM pulses under study could be induced by the slipping of two rough and rigid fBm profiles one over the other, or, equivalently, whether the EM activity behaves as a temporal fractal following the fBm model. The answer is positive. As it has been shown previously, the strong kHz EM fluctuations behave as a temporal fractal following the persistent fBm model, while their temporal profile has a roughness in harmony with the universal spatial roughness of the fracture surfaces.

An important pursuit is to make a further quantitative comparison between characteristics of the kHz EM time series on one hand and the self asperity model on the other hand. Two relevant arguments are the following.

First argument. The self-affine asperity model (Hallgass et al., 1997) suggests that the distribution of areas of the asperities broken A follows a power law

$$P(A) \sim A^{-\delta},$$

with an exponent δ which could be related to the Hurst exponent $0 < H < 1$ that controls the roughness of the fault. The former relation is obtained by supposing that the area of the broken asperities scales with its linear extension l as $A_{\mathrm{asp}} \sim l^{(1+H)}$.

The H-exponent associated with the kHz EM activity under study is distributed around the value 0.7. Based on the previously presented arguments it is reasonable to assume that in the case of the L'Aquila EQ the broken asperities scaled with its linear dimension l as $A_{\mathrm{asp}} \sim l^{1.7}$. Importantly, numerical studies performed by de Arcangelis et al. (1989) indicate that the number of bonds that break scales during the whole process of fracture as $l^{1.7}$ with the system size l. This consistency further supports the seismogenic origin of the anomalies under study.

Second argument. The self affine asperity model (Hallgass et al., 1997) also reproduces the Gutenberg-Richter law. More precisely, it suggests that a seismic event releases energy in the interval $[E, E+dE]$ with a probability $P(E)dE$, $P(E) \sim E^{-B}$, where $B = \alpha + 1$ and $\alpha = 1 - H/2$ with $\alpha \in [1/2, 1]$.

In the present case, the Hurst exponent $H \sim 0.7$ leads to $\alpha \sim 0.65$. Thus, the fracture of asperities released EM energies following the distribution $P(E) \sim E^{-B}$, where $B \sim 1.65$. This value is in harmony with both geophysical and laboratory data. Indeed, the distribution of energies released at any EQ is described by the power-law, $P(E) \sim E^{-B}$, where $B \sim 1.4 - 1.6$ (Gutenberg and Richter, 1954). On the other hand authors have presented experimental evidence in terms of acoustic emission which shows that the scaling law $P(E) \sim E^{-B}$ fits the data where $B \sim 1.5$ (Diodati et al., 1991), 1.3 ± 0.1 (Petri et al., 1994), 1.5 (Maes et al., 1998), 1.5 (Canneli et al., 1993) or 1.3-1.6 (Houle and Sethna, 1996). Notice that theoretical studies also lead to similar B-exponents (Kapiris et al., 2004b and references therein).

The above reported consistencies further bridge the kHz EM anomalies under study with the activation of the L'Aquila fault.

7 Detection of ionospheric perturbations associated with the L'Aquila EQ

EQ precursory signatures appear not only in the lithosphere, but also in the atmosphere and ionosphere (LAI coupling) (e.g, Hayakawa and Fujinawa, 1994; Molchanov and Hayakawa, 1998; Hayakawa, 1999; Hayakawa et al., 1999; Hayakawa and Molchanov, 2002; Pulinets and Boyarchuk, 2005; Muto et al., 2008). Both natural signals (atmospherics) and artificial EM signals propagate in the Earth-ionosphere waveguide. Any change in the lower ionosphere may result in significant changes in the signal received at a station. Especially, statistical analyses on the correlation between the lower ionospheric perturbations (as they detected by the ground-based reception of subionospheric EM waves from VLF/LF transmitters) have been performed by Rozhnoi et al. (2004) and Maekawa et al. (2006). The authors conclude that the lower ionosphere is definitely perturbed for the shallow EQs with magnitude larger than 6.0. Pulinets et al. (2003) have provided a strong evidence for occurrence of ionospheric precursors well before the main shock of EQ: ionospheric precursors within 5 days before the seismic shock were registered in 73% of the cases for EQs with magnitude 5 and in 100% of the cases for EQs with magnitude 6.

The L'Aquila EQ occurred in land was very shallow and its magnitude was 6.3. These parameters justify the appearance of pre-earthquake ionospheric perturbations. Indeed, a ULF EM anomaly possibly originated in an induced LAI coupling has been reported (see Fig. 5). During quiet periods, the daily ULF EM data presents a main bay-like behaviour (see Fig. 5). The records refer to the Earth-ionosphere waveguide propagation of natural EM emission that depends mostly on sources rooted in atmosphere and ionosphere (see p. 46 in ref. Gokhberg et al., 1995). The night time radiation is more intense than the day time radiation because the absorption in the D and E ionospheric layers decreases with the decreased density of electrons and ions at night. Any change in the lower ionosphere due to an induced pre-seismic LAI-coupling may result in significant changes in the signal propagation-received at a station. Thus, the emergence of an ULF anomaly is recognized by a strong perturbation of the characteristic bay-like morphology in the chain of daily ULF data. We observe such a pre-earthquake perturbation in the chain of daily ULF data. The anomaly was observed from 29 March 2009 up to 3 April 2009 (Fig. 5). The bay-like daily profile has been disappeared during this period.

The reproducibility of results is desirable in this field of research. Biagi et al. (2009), based on radio sounding, have observed an ionospheric anomaly. The intensities of MCO (f=216 kHz, France), CZE (f=270 kHz, Czech Republic), and CLT (f=189 kHz, Sicily, Italy) broadcast signals have been collected by a receiver operating in a place located about 13 km far from the EQ. From 31 March to 1 April the intensity of the MCO signal dropped and this drop was observed only in this signals. The anomaly is represented by the disappearance of the signal at day time and at night time.

Rozhnoi et al. (2009), based on very low frequency (kHz) radio sounding, have also reported that ionospheric perturbations appeared before the L'Aquila EQ. Using two known procedure of analysis, namely, revelation of night-time signal anomalies and anomalous shift in the evening terminator time, they have found clear anomalies in the time interval 2–8 days before the EQ occurrence.

We pay attention to the fact that our results show very close similarities in comparison to the anomalies observed by Biagi et al. (2009) and Rozhnoi et al. (2009) in terms of leading time.

A reliable manifestation of lithosphere-ionosphere coupling during the preparations of the L'Aquila EQ may further prove the assumption that an important part of energy, and thus seismogenic EM emission, was transmitted from the lithosphere into the atmosphere and further into the ionosphere.

8 Conclusions

ULF, MHz and kHz EM anomalies were detected prior to the L'Aquila EQ that occurred on 6 April 2009. The main goal of this work is to provide insight whether the observed anomalies were seismogenic or not.

A major class of seismo-EM signals is rooted in anomalous propagation of EM signals over epicentral regions associated with the variation of Earth-ionosphere wave-guide due to a pre-seismic LAI-coupling. The recorded ULF EM anomaly at Zante station from 29 March 2009 up to 3 April 2009 seems to fit in this category.

A second key class refers to EM signals believed to be emitted from within the focal zones (Uyeda et al., 2009). We argue that the detected MHz and kHz EM anomalies were emitted from within the focal zones. We have paid attention to the fact that the MHz radiation appears earlier than the kHz on both laboratory and geophysical scales (Eftaxias et al., 2002). We recently proposed the following two-stage model (Kapiris et al., 2004; Contoyiannis et al., 2005, 2008; Papadimitriou et al., 2008; Eftaxias et al., 2006, 2007b). The initially emerged MHz EM emission is thought to be due to the fracture of a highly heterogeneous system that surrounds a family of large high-strength asperities distributed along the fault sustaining the system. The finally emerged strong impulsive kHz EM radiation is due to the fracture of the asperities themselves. We show that the MHz and kHz EM candidate precursors follow the above mentioned scheme. The combination of the introduced criteria for recognition of EM anomalies as preseismic ones with the proposed two stages model of EQ preparation process increases the efficiency of the proposed scheme. It is attractive that the suggested criteria include only universal parameters and do not involve physical and mechanical parameters of materials which are beyond the control of the researcher.

The new field of study of complex systems holds that the dynamics of complex systems are founded on universal principles that may used to describe disparate problems. A basic reason for our interest in "complexity" is the striking similarity in behavior near the global instability among systems that are otherwise quite different in nature (Stanley, 1999, 2000; Sornette, 2002). A corollary is that transferring ideas and results from investigators in hitherto disparate areas will cross-fertilize and lead to important new results. Experimental evidence supports the possibility that kHz preseismic EM emissions, earthquakes, magnetic storms, solar flares, and epileptic seizures have certain quantitative features that are intriguingly similar. Indeed, results show that all the crucial features extracted from the pre-seismic kHz EM activity under study (Eftaxias et al., 2009b), including high organization and persistency, are also contained in intense magnetic storms (Balasis et al., 2006, 2008, 2009) and epileptic seizures (Kapiris et al., 2005; Eftaxias et al., 2006). We have suggested that the development of kHz EM precursors, intense magnetic storms and epileptic seizures can study within a unified framework, e.g., Intermittent Criticality, which has a more general character than classical Self-Organized (Balasis et al., 2006; Kapirirs et al., 2005; Eftaxias et al., 2006). Recently, we showed that the modified non-extensive Gutenberg-Richter type law (7) is also able to describe the distribution of magnitude of magnetic storms (Balasis and Eftaxias, 2009) and solar flares (Eftaxias et al., 2009c) by a similar q parameter. Thus, the detected kHz EM precursor shows striking similarity in behavior near the global instability with extreme events that are otherwise quite different in nature, as it is predicted by the theory of complex systems.

Whether the presented ideas will prove to be universal or disappear as others, will turn out in the future. The complexity of pre-seismic EM activities generation is enormous, and thus a huge amount of research is needed before we begin to understand it.

Acknowledgements. We thank Natalia Smirnova for useful comments and constructive remarks.

Edited by: M. Hayakawa
Reviewed by: N. A. Smirnova and another anonymous referee

References

Bahat, D., Rabinovitch, A., and Frid, V.: Tensile fracturing in rocks: Tectonofractographic and Electromagnetic Radiation Methods, Springer Verlag, Berlin, 570 pp., 2005.

Balasis, G., Daglis, I. A., Kapiris, P., Mandea, M., Vassiliadis, D., and Eftaxias, K.: From pre-storm activity to magnetic storms: a transition described in terms of fractal dynamics, Ann. Geophys., 24, 3557–3567, 2006, http://www.ann-geophys.net/24/3557/2006/.

Balasis, G., Daglis, I., Papadimitriou, C., Kalimeri, M., Anastasiadis, A., and and Eftaxias, K.: Dynamical complexity in *Dst* time series using non-extensive Tsallis entropy, Geophys. Res. Lett., 35, L14102, doi:10.1029/2008GL034743, 2008.

Balasis, G. and Eftaxias, K.: A study of non-extensivity in the Earth's magnetosphere, Eur. Phys.l J.-Spec. Top., 174, 219-225, 2009.

Balasis, G., Daglis, I., Papadimitriou, C., Kalimeri, M., Anastasiadis, A., and Eftaxias, K.: Investigating dynamical complexity in the magnetosphere using various entropy measures, J. Geophys. Res., 114, A00D06, doi:10.1029/2008JA014035, 2009.

Barriere, B. and Turcotte, D. L.: A Scale-Invariant Cellular-Automata Model for Distribited Seismicity, Geophys. Res. Lett., 18, 2011-2014, 1991.

Biagi, P. F., Castellana, L., Maggipinto, T., Loiacono, D., Schiavulli, L., Ligonzo, T., Fiore, M., Suciu, E., and Ermini, A.: A pre seismic radio anomaly revealed in the area where the Abruzzo earthquake (M=6.3) occurred on 6 April 2009, Nat. Hazards Earth Syst. Sci., 9, 1551–1556, 2009, http://www.nat-hazards-earth-syst-sci.net/9/1551/2009/.

Bouchon, M.: The state of stress on some faults of the San Andreas system as inferred from near-field strong motion data, J. Geophys. Res., 102, 11731-11744, 1997.

Cannelli, G., Cantelli, R., and Cordero, F.: Self-organized criticality of the fracture processes associated with hydrogen precipitation in niobium by acoustic emission, Phys. Rev. Lett., 70, 3923-3926, 1993.

Carvalho, J., Silva, R., do Nascimento Jr., J., and De Medeiros, J.: Power law statistics and stellar rotational velocities in the Pleiades, Eur. Phys. Lett., 84, 59001/16, doi: 10.1209/0295-5075/84/59001, 2008.

Chakrabarti, B. and Stinchocombe, R.: Stick-slip statistics for two fractal surfaces: a model for earthquakes, Physica A, 270, 27-34, 1999.

Contoyiannis, Y. and Diakonos, F.: Criticality and intermittency in the order parameter space, Phys. Lett. A, 268, 286–272, 2000.

Contoyiannis, Y., Diakonos, F., and Malakis, A.: Intermittent dynamics of critical fluctuations, Phys. Rev. Lett., 89, 35701–35704, 2002.

Contoyiannis, Y., Diakonos, F., Papaefthimiou, G., and Theophilidis, G.: Criticality in the Relaxation Phase of the Spontaneous Contracting Atria Isolated From the Heart of the Frog (Rana Ridibunda), Phys. Rev. Lett., 93, 098101, 1–4, 2004.

Contoyiannis, Y., Kapiris, P., and Eftaxias, K.: Monitoring of a preseismic phase from its electromagnetic precursors, Phys. Rev. E, 71, 061123, 1–14, 2005.

Contoyiannis, Y. F. and Eftaxias, K.: Tsallis and Levy statistics in the preparation of an earthquake, Nonlin. Processes Geophys., 15, 379–388, 2008, http://www.nonlin-processes-geophys.net/15/379/2008/.

Contoyiannis, Y., Nomicos. C., Kopanas, J., Antonopoulos, G., Contoyianni, L., and Eftaxias, K.: Critical features in electromagnetic anomalies detected prior to the L'Aquila earthquake, Physica A, 389, 499–508, 2009.

Corral, A., Perez, C., and Diaz-Guilera, A.: Self-organized criticality induced by diversity, Phys. Rev. Lett., 78(8), 1492-1495, 1997.

Cyranoski, D.: A seismic shift of thinking, Nature, 431, 1032–1034, 2004.

Diakonos, F., Pingel, D., and Schmelcher, P.: A stochastic approach to the construction of one-dimensional chaotic maps with prescribed statistical properties, Phys. Lett. A, 264, 162–170. 1999.

Diodati, P., Marchesoni, F., and Piazza, S.: Acoustic emission from volcanic rocks: An example of self-organized criticality, Phys. Rev. Let., 67, 2239-2241, 1991.

Eftaxias, K., Kopanas, J., Bogris, N., Kapiris, K., Antonopoulos, G., and Varotsos P.: Detection of electromagnetic earthquake precursory signals in Greece, P. Jpn. Acad. B.-Phys., 76, 45–50, 2000.

Eftaxias, K., Kapiris, P., Dologlou, E., Kopanas, J., Bogris, N., Antonopoulos, G., Peratzakis, A., and Hadjicontis, V.: EM anomalies before the Kozani earthquake: A study of their behaviour through laboratory experiments, Geophys. Res. Lett., 29, 69/1–69/4, 2002.

Eftaxias, K., Frangos, P., Kapiris, P., Polygiannakis, J., Kopanas, J., Peratzakis, A., Skountzos, P., and Jaggard, D.: Review and a Model of Pre-Seismic electromagnetic emissions in terms of fractal electrodynamics, Fractals, 12, 243–273, 2004.

Eftaxias, K. A., Kapiris, P. G., Balasis, G. T., Peratzakis, A., Karamanos, K., Kopanas, J., Antonopoulos, G., and Nomicos, K. D.: Unified approach to catastrophic events: from the normal state to geological or biological shock in terms of spectral fractal and nonlinear analysis, Nat. Hazards Earth Syst. Sci., 6, 205–228, 2006, http://www.nat-hazards-earth-syst-sci.net/6/205/2006/.

Eftaxias, K., Sgrigna, V., and Chelidze, T.: Mechanical and Electromagnetic Phenomena Accompanying Preseismic Deformation: from Laboratory to Geophysical Scale, Tectonophysics, 431, 1-301, 2007a.

Eftaxias, K., Panin, V., and Deryugin Y.: Evolution EM-signals before earthquake and during laboratory test of rocks, Tectonophysics, 431, 273-300, 2007b.

Eftaxias, K.: Footprints of nonextensive Tsallis statistics, selfaffinity and universality in the preparation of the L'Aquila earthquake hidden in a pre-seismic EM emission, Physica A, 389, 133–140, 2009a.

Eftaxias, K., Athanasopoulou, L., Balasis, G., Kalimeri, M., Nikolopoulos, S., Contoyiannis, Y., Kopanas, J., Antonopoulos, G., and Nomicos, C.: Unfolding the procedure of characterizing recorded ultra low frequency, kHZ and MHz electromagetic anomalies prior to the L'Aquila earthquake as pre-seismic ones - Part 1, Nat. Hazards Earth Syst. Sci., 9, 1953–1971, 2009b, http://www.nat-hazards-earth-syst-sci.net/9/1953/2009/.

Eftaxias, K., Balasis, G., Papadimitriou, C., and Mandea, M.: Universality in solar flares, magnetic storms, earthquakes and pre-seismic electromagnetic emissions by means of nonextensivity, AGU Fall Meeting, 2009c.

Freund, F., Takeuchi, A., and Lau, B.: Electric current streaming out of stressed igneous rocks - a step towards understanding pre-earthquake low frequency EM emissions, Phys. Chem. Earth, 31, 389–396, 2006.

Gershenzon, N. and Bambakidis, G.: Modelling of seismoelectromagnetic phenomena, Russian Journal of Earth Sciences, 3, 247–275, 2001.

Gokhberg, M., Morgounov, V., and Pokhotelov, O.: Earthquake Prediction, Seismo-Electromagnetic Phenomena, Gordon and Breach Publishers, 1995.

Gusev, A.: On relation between earthquake population and asperity population on the fault, Tectonophysics, 211, 85-98, 1992.

Gutenberg, B. and Richter, C.: Seismicity of the Earth and Associated Phenomena, 2nd edn., Princeton Univ. Press, Princeton, New Jersey, USA,, 310 pp. 1954.

Hadjicontis, V., Mavromatou, C., Antsygina, T., and Chisko, K.: Mechanism of electromagnetic emission in plastically deformed ionic crystals, Phys. Rev. B, 76, 024106/1–14, 2007.

Hallgass, R., Loreto, V., Mazzella, O., Paladin, G., and Pietronero, L.: Self-affine model of earthquakes, Phys. Rev. Lett., 76, 2599-2562, 1997.

Hansen, A. and Schmittbuhl, J.: Origin of the universal roughness exponent of brittle fracture surfaces: stress-weighted percolation in the damage zone, Phys. Rev. Lett., 90, 45504-45507, 2003.

Hayakawa, M. and Fujinawa, Y.: Electromagnetic Phenomena Related to Earthquake Prediction, Terrapub, Tokyo, 1994.

Hayakawa, M.: Atmospheric and Ionospheric Electromagnetic Phenomena Associated with Earthquakes, Terrapub, Tokyo, 1999.

Hayakawa, M., Itoh, T., and Smirnova, N.: Fractal analysis of ULF geomagnetic data associated with the Guam earthquake on August 8, 1993, Geophys. Res. Lett., 26(18), 2797–2800, 1999.

Hayakawa, M. and Molchanov, O.: Seismo Electromagnetics, Terrapub, Tokyo, 2002.

Henegham, C. and McDarby, G.: Establishing the relation between detrended fluctuation analysis and power spectral density analysis foe stochastic processes, Phys. Rev. E, 62, 6103–6110, 2000.

Herrmann, H. J. and Roux, S.: Statistical Physics for the Fracture of Disordered Media, Elsevier, Amsterdam, 1990.

Houle, P. and Sethna, J.: Acoustic emission from crumpling paper, Phys. Rev. E, 54, 278-283, 1996.

Huang, J. and Turcotte, D.: Fractal distributions of stress and strength and variations of bvalue, Earth Planet. Sc. Lett., 91, 223-230, 1988.

Hurst, H.: Long term storage capacity of reservoirs, T. Am. Soc. Civ. Eng., 116, 770-808, 1951.

Ida, Y., Hayakawa, M., Adalev, A., and Gotoh, K.: Multifractal analysis for the ULF geomagnetic data during the 1993 Guam earthquake, Nonlin. Processes Geophys., 12, 157–162, 2005, http://www.nonlin-processes-geophys.net/12/157/2005/.

Kagan, Y. and Knopoff, L.: Spatial distribution of earthquakes: the two-point correlation function, Geophys. J. Roy. Astr. S., 62, 303-320, 1980.

Kalimeri, M., Papadimitriou, K., Balasis, G., and Eftaxias, K.: Dynamical complexity detection in pre-seismic emissions using nonadditive Tsallis entropy, Physica A, 387, 1161-1172, 2008.

Kapiris, P., Eftaxias, K., and Chelidze, T.: The electromagnetic signature of prefracture criticality in heterogeneous media, Phys. Rev. Lett., 92, 065702.1–4, 2004a.

Kapiris, P. G., Balasis, G. T., Kopanas, J. A., Antonopoulos, G. N., Peratzakis, A. S., and Eftaxias, K. A.: Scaling similarities of multiple fracturing of solid materials, Nonlin. Processes Geophys., 11, 137–151, 2004b, http://www.nonlin-processes-geophys.net/11/137/2004/.

Kapiris, P., Polygiannakis, J., Li, X., Yao, X., and Eftaxias, K.: Similarities in precursory features in seismic shocks and epileptic seizures, Europhys. Lett. 69, 657–663, 2005.

Karamanos, K., Dakopoulos, D., Aloupis, K., Peratzakis, A., Athanasopoulou, L., Nikolopoulos, S., Kapiris, P., and Eftaxias, K.: Study of pre-seismic electromagnetic signals in terms of complexity, Phys. Rev. E, 74, 016104, 21 pp., 2006.

Kossobokov, V.: Testing earthquake prediction methods: the West Pacific short-term forecast of earthquakes with magnitude MwHRV¿5.8, Tectonophysics, 413, 25–31, 2006

Koulouras, G., Balasis, G., Kiourktsidis, I., Nannos, E., Kontakos, K., Stonham, J., Ruzhin, Y., Eftaxias, K., Kavouras, D., and Nomikos, K.: Discrimination between preseismic electromagnetic anomalies and solar activity effects, Phys. Scripta, 79, 45901, 12 pp., 2009.

Lei, X. and Satoh, T.: Indicators of critical point behaviour priot to rock failure inferred from pre-failure damage, Tectonophysics, 431, 97–111, 2007.

Lopez, J. and Schmittbuhl, J.: Anomalous scaling of fracture surfaces, Phys. Rev. E, 57, 6405–6408, 1998.

Maekawa, S., Horie, T., Yamauchi, T., Sawaya, T., Ishikawa, M., Hayakawa, M., and Sasaki, H.: A statistical study on the effect of earthquakes on the ionosphere, based on the subionospheric LF propagation data in Japan, Ann. Geophys., 24, 2219–2225, 2006, http://www.ann-geophys.net/24/2219/2006/.

Maes, C., Moffaert, A., Frederix, H., and Strauven, H.: Criticality in creep experiments on cellular glass, Phys. Rev. B, 57, 4987-4990, 1998.

Mandelbrot, B.: The Fractal Geometry of Nature, W. H. Freeman, New York, USA, 486 pp., 1982.

Maslov, S., Paczuski, M., and Bak, P.: Avalanches and 1/f Noise in Evolution and Growth Models, Phys. Rev. Lett., 73(16), 2162–2165, 1994.

Molchanov, O. A. and Hayakawa, M.: Seismo-Electromagnetics and Related Phenomena: History and latest results, TERRAPUB, 189 pp., 2008.

Mourot, G., Morel, S., Bouchaud, E., and Valentin, G.: Scaling properties of mortar fracture surfaces, Int. J. Fracture, 140, 39-54, 2006.

Muto, J., Nagahama, H., Miura, T., and Arakawa, I.: Frictional discharge at fault asperities: origin of fractal seismo-electromagnetic radiation, Tectonophysics, 431, 113–122, 2007.

Muto, F., Yoshida, M., Horie, T., Hayakawa, M., Parrot, M., and Molchanov, O. A.: Detection of ionospheric perturbations associated with Japanese earthquakes on the basis of reception of LF transmitter signals on the satellite DEMETER, Nat. Hazards Earth Syst. Sci., 8, 135–141, 2008, http://www.nat-hazards-earth-syst-sci.net/8/135/2008/.

Ohnaka, M. and Shen, L.: Scaling of the shear rupture from nuvleation to dynamic propagation: Implications of geometry irregularity of the rupture surfaces, J. Geophys. Res., 104, 817–844, 1999.

Papadimitriou, C., Kalimeri, M., and Eftaxias, K.: Nonextensivity and universality in the earthquake preparation process, Phys. Rev. E., 77, 036101/1-14, 2008.

Petri, A., Paparo, G., Vespignani, A., Alippi, A., and Constantini, M.: Experimental evidence for critical dynamics in microfracturing processes, Phys. Rev. Let, 73, 3423-3426, 1994.

Peyrat, S., Olsen, K., and Madariaga, R.: Dynamic modeling of the 1992 Landers earthquake, J. Geophys. Res., 106, 26467-26482, 2001.

Pingel, D., Schmelcher, P, and Diakonos, F.: Theory and examples of the inverse Frobenius-Perron problem for complete chaotic maps, Chaos, 9, 357–372, 1999.

Ponomarev, A., Zavyalov, A., Smirnov, V., and Lockner, D.: Physical modelling of the formation and evolution of seismically active fault zones, Tectonophysics, 277, 57–81, 1997.

Ponson, L., Bonamy, D., and Bouchaud, E.: Two-dimensional scaling properties of experimental fracture surfaces, Phys. Rev. Lett., 96(3), 035506, doi:10.1103/PhysRevLett.96.035506, 2006.

Power, W., Tullis, T., Brown, S., Boitnott, G., and Scholz, C.: Roughness of the natural faults surfaces, Geophys. Res. Lett., 14, 29–32, 1987.

Pulinets, S. and Legen'ka, A.: Dynamics of the near-equatorial ionosphere prior to strong earthquakes, Geomagn. Aeronomy+, 42, 227–232, 2002.

Pulinets, S., Legen'ka, A., Gaivoronskaya, T., and Depuev, V: Main phenomenological of ionospheric precursors of strong earthquakes, J. Atmos. Sol.-Terr. Phy., 65, 1337–1347, 2003.

Pulinets, S. and Boyarchuk, K.: Ionospheric Precursors of Earthquakes, Springer, 316 pp., 2005.

Pulinets, S: Physical mechanism of the vertical electric field generation over active tectonic faults, Adv. Space Res., 44, 767–773, 2009.

Qian, S., Yian, J., Cao, H., Shi, S., Lu, Z., and Ren, K.: Results of the observations on seismo-electromagnetic waves at two earthquake experimental areas in China, in: Electromagnetic Phenomena Related to Earthquake Prediction, edited by: Hasyakawa, M. and Fujinawa, Y., TerraPub, Tokyo, 205–211, 1994.

Rabinovitch, A., Frid, V., and Bahat, D.: Gutenberg-Richter-type relation for laboratory fracture-induced electromagnetic radiation, Phys. Rev. E, 65, 11401/1–11401/4, 2001.

Renard, F., Voisin, C., Marsan, D., and Schmittbuhl, J.: High resolution 3D laser scanner measurements of a strike-slip fault quantify its morphological anisotropy at all scales, Geophys. Res. Lett., 33, L04305, doi:10.1029/2005GL025038, 2006.

Roznoi, A., Solovieva, M., Molchanov, O., and Hayakawa, M.: Middle latitude LF (40 kHz) phase variations associated with earthquakes for quiet and disturbed geomagnetic conditions, Phys. Chem. Earth, 29, 589–598, 2004.

Rozhnoi, A., Solovieva, M., Molchanov, O., Schwingenschuh, K., Boudjada, M., Biagi, P., Maggipinto, T., and Castellana, L: VLF signal precursor of L'Aquila earthquake. JRA3/EMDAF kick-off meeting, 2009.

De Rubeis, V., Hallgass, R., Loreto, V., Paladin, G., Pietronero, L., and Tosi, P.: Self-affine model of earthquakes, Phys. Rev. Lett. 76, 2562-2599, 1996.

Rundle, J., Turcotte, D., Shcherbakov, R., Klein, W., and Sammis, C.: Statistical physics approach to understanding the multiscale dynamics of earthquake fault systems, Rev. Geophys., 41(4), 5/1–30, 2003.

Silva, R., Franca, G., Vilar, C., and Alcaniz, J.: Nonextensive models for earthquakes, Phys. Rev. E, 73, 026102, 1–5, 2006.

Sammis, C. and Sornette, D.: positive feedback, memory, and the predictability of earthquakes, P. Natl. Acad. Sci. USA, 99, 2501–2508, 2002.

Smirnova, N., Hayakawa, M., Gotoh, K., and Volobuev, D.: Scaling characteristics of ULF geomagnetic fields at the Guam seismoactive area and their dynamics in relation to the earthquake, Nat. Hazards Earth Syst. Sci., 1, 119–126, 2001, http://www.nat-hazards-earth-syst-sci.net/1/119/2001/.

Solotongo-Costa, O. and Posadas, A.: Fragment-asperity interaction model for EQ, Phys. Rev. Lett., 92, 048501, 1–4, 2004.

Sornette D. and A. Helmstetter.: Occurrence of finite-time singularities in epidemic models of rupture, EQ, and starquakes, Phys. Rev. Lett., 89, 158501, 1–4, 2002.

Sornette, D.: Critical Phenomena in Natural Sciences, Chaos, Fractals, Self-organization and Disorder: Concepts and Tools, Second edition, Springer Series in Synergetics, Heidelberg, 2004.

Stanley, H. E.: Scaling, universality, and renormalization: three pillars of modern critical phenomena, Rev. Mod. Phys., 71, 358–366, 1999.

Tsallis, C.: Possible generalization of Boltzmann-Gibbs statistics, J. Stat. Phys., 52, 479-487, 1988.

Tsallis, C.: Introduction to Nonextensive Statistical Mechanics, Approaching a Complex Word, Springer, 2009.

Turcotte, D.: Fractals and chaos in geology and geophysics, 2nd edn., Cambridge University Press, 398 pp., 1997.

Uyeda, S., Nagao, T., Orihara, Y., Yamaguchi, T., and Takahashi, I.: Geoelectric potential changes: possible precursors in Japan, P. Natl. Acad. Sci. USA, 97, 4561–4556, 2000.

Uyeda, S., Nagao, T., and Kamogawa, M.: Short-term earthquake prediction: Current status of seismo-electromagnetics, Tectonophysics, 470, 205–213, 2009.

Varotsos, P.: The Physics of Seismic Electric Signals, TerraPub, Tokyo, 2005.

Vilar, C., Franca, G., Silva, R., and Alcaniz, J.: Nonextensivity in geological faults?, Physica A, 377, 285–290, 2007.

Walters, R., Elliot, J., D Agostino, N., England, P., Hunstad, I., Jackson, J., Parsons, B., Phillips, R., and Roberts, G.: The 2009 L'Aquila earthquake (central Italy): A source mechanism and implications for seismic hazard, Geophys. Res. Lett., 36, L17312, doi:10.1029/2009GL039337, 2009.

Zapperi, S., Kumar, P., Nukala, V., and Simunovic, S.: Crack roughness and avalanche precursors in the random fuse model, Phys. Rev. E, 71, 26106/1-10, 2005.

Zunino, L., Perez, D., Kowalski, A., Martin, M., Garavaglia, M., Plastino, A., and Rosso, O.: Fractional Brownian motion, fractional Gaussian noise, and Tsallis permutation entropy, Physica A, 387, 6057–6088, 2008.